Atmospheric
Chemistry
and Physics
Discussions

Open Access

1 **Impact of VOCs on the formation of ozone in a central China city during severe pollution**

2 **periods**

3 Bowei Li[1], Steven Sai Hang Ho[2,3*], Sunling Gong[1,4*], Jingwei Ni[1], Huairui Li[1], Liyan Han[1], Yi

4 Yang[1], Yijin Qi[1], Dongxu Zhao[1]

5 [1] *Langfang Academy of Eco Industrialization for Wisedom Environment, Langfang 065000, China*

6 [2] *Division of Atmospheric Sciences, Desert Research Institute, Reno, Nevada, USA*

7 [3] *Key Lab of Aerosol Chemistry & Physics, Institute of Earth Environment, Chinese Academy of*

8 *Sciences, Xi'an 710061, China*

9 [4] *Center for Atmosphere Watch and Services of CMA, Chinese Academy of Meteorological Sciences,*

10 *Beijing 100081, China*

11 *Correspondence to: Steven Sai Hang Ho (stevenho@hkpsrl.org) and Sunling Gong

12 (gongsl@cma.gov.cn)

Atmospheric
Chemistry
and Physics
Discussions
Open Access
EGU

13    **Abstract**

14    In this work, a five-month sampling campaign was conducted ~~for~~ volatile organic compounds

15    (VOCs) for the first time in Zhengzhou City, Henan province, China, where ozone ($O_3$) pollution

16    has shown an increasing trend in recent years. Fifty-seven VOCs defined by the Photochemical

17    Assessment Monitoring Stations (PAMS) were sampled using canister method. ~~Meanwhile, other~~

18    $O_3$ precursor gases were monitored online at four different sites ~~between the time period of May~~

19    ~~September, 2017~~. The results indicated that the average mixing ratio of $\Sigma_{PAMS}$ (31.57±23.35 ppbv)

20    in Zhengzhou was lower than the other megacities in China, while alkyne was in a significantly

21    higher proportion. The abundances, compositions and ratios of PAMS showed strong spatial and

22    temporal variations. Alkenes were the largest contributors to ~~the~~ ozone formation potential (OFP).

23    On clear days, higher $O_3$ levels were often accompanied with high $\Sigma_{PAMS}/NO_x$ ratio at each site,

24    demonstrating that the VOCs were more sensitive during the $O_3$ formation period in Zhengzhou.

25    Furthermore, source apportionmemt was conducted with Positive Matrix Factorization (PMF)

26    ~~model~~, and it was found that ~~the use of~~ compressed natural gas (CNG), the evaporation of gasoline

27    and the exhaust from vehicles were the important sources for ambient VOCs at all four sites.

28    ~~Besides,~~ ~~the~~ meterological conditions and long-range transport from other surrounding provinces

29    also had an impact on the air quality ~~determined using~~ the cluster analysis. It is worth mentioning

30    that the reduction in VOCs' emissions is necessary to suppress the $O_3$ pollution.

31

32    **1. Introduction**

33    Volatile organic compounds (VOCs) are diverse and reactive chemicals. Vehicle exhausts, fuel

34    combustion and evaporation, and solvent usage are the known major anthropogenic sources of

35    VOCs (Zhang et al., 2014;Yan et al., 2017;Wang et al., 2013a;Liu et al., 2017;Sahu et al., 2017).

36    Since VOCs play a crucial role in the formation of ground-level ozone ($O_3$) and secondary organic

37    aerosol (SOA) (Yuan et al., 2013a;Han et al., 2018;Wang et al., 2018), studies on VOCs are being

38    conducted globally (Wei et al., 2014;Malley et al., 2015;Ou et al., 2015;Zhu et al., 2017;Zhao et al.,

39    2015). Fifty-seven VOCs, including $C_2$ - $C_{10}$ alkanes, alkenes, alkynes and aromatics, which greatly

40    contribute to ambient $O_3$, have been defined and regularly monitored by Photochemical Assessment

41    Monitoring Stations (PAMS) (Shao et al., 2016;Chen et al., 2010). With the rapid economic

42    development, $O_3$ pollution has troubled all urban cities (Wang et al., 2017c;Nagashima et al., 2017).

43    Non-linearity relationships between the ambient VOCs, nitrogen oxide ($NO_x$) and $O_3$ production

44    indicate that the reduction in tropospheric $O_3$ is complex (Lin et al., 1998;Hidy and Blanchard,

45    2015;Li et al., 2018). During the time period of 1960 - 2010, the concentrations of VOCs and $NO_x$

46    have decreased at the rate of 7.3% $yr^{-1}$ and 2.6% $yr^{-1}$, respectively, due to which, the $O_3$ extrema

47    declined in southern California (Pollack et al., 2013). Evaluations on the production efficiency of

48    $O_3$ suggested the increase in responsiveness of $O_3$ to $NO_x$ in southeastern U.S, and therefore, the

49    changes in anthropogenic emissions of VOCs should be taken into consideration (Blanchard and

50    Hidy, 2017). Many modeling and field studies proved that photochemical production of $O_3$ in

51    several regions in China, such as Guangzhou, Shanghai and Beijing, were sensitive to VOCs (Shao

52    et al., 2009;Gao et al., 2017;Ou et al., 2016), and the sensitivity regime was always in flux

53    (Luecken et al., 2018). It is predicted that the formation regime of $O_3$ will be more sensitive to

54    VOC emissions in China by 2030 (Jin and Holloway, 2015), On the other hand, the International

55    Agency for Research on Cancer (IARC, 2017) has identified several VOCs, such as benzene and

56    1,3-butadiene as the first class carcinogens (Hoque et al., 2008;Iannuzzi et al., 2010).

57        In recent years, investigations involving the source apportionment of VOCs, acquirement of

58    emission profiles and interpretation of the seasonal variations in China were mainly concentrated in

59    Yangtze River Delta (YRD), Pearl River Delta (PRD) and Beijing-Tianjin region (BJT) (An et al.,

60    2014;Wang et al., 2014;Chen et al., 2014;Liu et al., 2016a;Guo et al., 2017). With the nationwide

61    deterioration of air quality, studies in less developed or developing regions, such as southwestern

62    and northwestern China, are scarce. Contributions from the burning of biomass and high

63    abundances of toxics and reactive compounds (such as, benzene) are prominent in these areas (Li et

64    al., 2014;Li et al., 2017a). Consequently, differences on the structure and reactivity of VOCs, which

65    render them different abilities to influence the production of ozone, and reactivity based on the air

66    quality control measures, have developed (Capps et al., 2012). Additionally, U.S. Environmental

67    Protection Agency (EPA) (2005) has encouraged states to take this approach while developing the

Atmospheric
Chemistry
and Physics
Discussions

68      Ozone State Implementation Plans (OSIP). Aromatics and alkenes were responsible for most of the

69      weighted reactivity of VOCs (59.4% and 25.8%, respectively) in PRD (Ou et al., 2015). With the

70      changes in energy infrastructure, industrial construction and meteorological conditions (Wang et al.,

71      2015;Shao et al., 2011), major emission sources of active compounds vary accordingly. For

72      example, in less developed cities, such as Heilongjiang and Anhui, the combustion of biomass had

73      the highest contribution to $O_3$ formation (40% and 36%, respectively), while in developed regions,

74      such as Shanghai, Beijing and Zhejiang, the solvent use became more important with time (>20%)

75      (Wu and Xie, 2017). Identifying the local chemical species play vital role in $O_3$ formation and

76      provides useful information for policy-makers to make strategies to alleviate $O_3$ pollution.

77      Zhengzhou is an important developing city in the mid-west of Huanghe-Huaihe river flood

78      plain in China. As the capital city of Henan province, it is densely populated with more than seven

79      million residents in 2010 (Geng et al., 2013). With the rapid growth of industrial activities, vehicle

80      emissions and fuel combustion, air quality in Zhengzhou has notoriously deteriorated. Zhengzhou is

81      categorized as one of the most polluted cities due to ~~the reason that on 65% of days in a year,~~ its air

82      quality exceeds the allowable limits set by Air Quality Guideline in 2013. ~~The city has the third~~

83      ~~worst air quality among 74 nationwide cities in the first half year of 2015.~~ Particularly, $O_3$ was the

84      most critical pollutant in Zhengzhou in 65 - 85 days of summer (Shen et al., 2017;Gong et al.,

85      2017). Over 50% of the days in a year, the mixing ratio of $O_3$ exceeded the Grade I standard of

86      daily maximum average 8-hour (DMA8) (100 μg m$^{-3}$) in Henan, while the estimated mortality of

87      chronic obstructive pulmonary disease (COPD), caused by $O_3$, was also higher compared to other

88      provinces in China (Liu et al., 2018). As the major precursors of $O_3$, the study on VOCs is of

89      significance. ~~However, for the city of Zhengzhou (China), the related research is non-existent in~~

90      ~~literature.~~ In this work, a comprehensive sampling campaign aiming at VOCs has been conducted at

91      four monitoring stations during the time period of May - September 2017. The spatial and temporal

92      variations in VOCs in Zhengzhou were determined. The contributions of major emission sources

93      were quantified, and the relationship between $O_3$-VOCs-$NO_x$ was discussed in detail. The results

94      and implications from this study can provide useful guidance for policy-makers to alleviate ozone

95      pollution in Zhengzhou, China.

Atmospheric
Chemistry
and Physics
Discussions

## 2. Experimental

### 2.1 Sampling site

According to the population density and industrial facilities, and in combination with the prevailing southeastern wind, four sites have been selected for the sampling campaign. These sites are Jingkai community (JK; 113.73°E, 34.72°N), municipal environmental monitoring station (MEM; 113.61°E, 34.75°N), Yinhang school (YH; 113.68°E, 34.80°N) and Gongshui company (GS; 113.57°E, 34.81°N), which are located at the southeastern, southwestern, northeastern and northwestern of urban Zhengzhou, respectively (Fig. 1). There was a main airport highway and heavy-traffic ring roads approximately 500 m west of JK. Furthermore, the site was at a distance of 2 km from an industrial area, which involved packaging and printing plants, and material distribution factories. It is noteworthy that there were three coal power plants in the urban area of Zhengzhou city. One of the power plants with the highest production was 1.6 km northwest of MEM. Both the MEM and YH included a mix of commercial and condensed residential areas, whereas the apartments around YH were more aged. In addition, GS was surrounded by several manufacturing plants, including pharmaceuticals, materials, foods and machineries.

Ten sampling days with the rainfall record (*ca*. 0 mm) were chosen in every month during the period of May - September, 2017. Pre-evacuated stainless-steel canisters (Entech Instrument, Inc., Simi Valley, CA, USA), each having the volume of 3.2 L, were used to instantaneously collect VOCs. Two samples, one collected at 07:00 and the other at 14:00, were obtained on every sampling day. There were a total of 400 valid samples collected in this study. The chemical analysis was accomplished within two weeks after the collection of samples. Real-time data for trace gases, including $SO_2$, $CO$, $NO_2$ and $O_3$, and synchronous meteorological data, such as temperature (T), relative humidity (RH), wind direction (WD) and wind speed (WS), were recorded at each air monitoring station.

### 2.2 Chemical Analysis

In this study, the measurement of VOCs was based on Compendium Method TO-15, which was established by U.S. EPA. Air in the canister was concentrated using liquid-nitrogen at -160 °C

Atmospheric
Chemistry
and Physics
Discussions

Open Access

EGU

123    in a cryogenic pre-concentrator (7100A, Entech Instrument, Inc.). Both the $CO_2$ and $H_2O$ were

124    removed from the transfer line. The air was then thermally desorbed at 120 °C and transferred for

125    analysis in a gas chromatography (GC, 7890A, Agilent Technologies, Santa Clara, CA, USA)

126    coupled with mass spectrometric detector (MSD)/flame ionization detector (FID) (5977E, Agilent

127    Technology). Dual columns and detectors were applied for the simultaneous analysis of $C_2$ - $C_{11}$

128    hydrocarbons. A PLOT column with the length of 15 m, internal diameter of 0.32 mm and film

129    thickness of 3.0 μm was connected to the FID for detection of $C_2$ - $C_5$ NMHCs, whereas $C_5$ - $C_{10}$

130    NMHCs, oxygenated VOCs (OVOCs) and halocarbons were separated using a DB-624 (30 m ×

131    0.25 mm inner diameter × 3.0 μm film thickness), which was connected to the MSD. The oven

132    temperature of GC was programed to the initial temperature of 37 °C for 5 min, which was

133    increased at the rate of 5 °C/min to 120 °C, and maintained at this temperature for 5 min. It was

134    then ramped at the rate of 6 °C/min to the final temperature of 180 °C, where it was maintained for

135    5 min. The total run time was 41.6 minutes. The MSD was operated with the electron ionization (EI)

136    impact (70 eV), where the ions were detected in the selected ion monitoring (SIM) mode. Based on

137    the retention time and mass spectra involving accurate standard, the targeted VOCs were identified,

138    and then, quantified using multi-point calibration curve. Three standard gases for TO-15 and PAMS

139    (1 ppm; Spectra Gases Inc, NJ, USA) were used. A total of 101 compounds, including 28 alkanes,

140    11 alkenes, 17 aromatics, 34 halocarbons, 9 OVOCs, acetylene and $CS_2$ were quantified. This study

141    discussed only 57 PAMS due to their critical role in $O_3$ pollution. Detailed information on the

142    PAMS involved in this study and their corresponding linearity of calibration ($R^2$), measurement

143    relative standard deviation (RSD), method detection limit (MDL), maximum increment reactivity

144    (MIR, carter, 2010) are presented in Table 1.

145    **2.3 Quality control and quality assurance (QC/QA)**

146    QC/QA was thoroughly executed to ensure the quality of research and obtain trustworthy

147    experimental data. In order to alleviate contamination from previous samples, canisters had to be

148    repeatedly cleaned using humidified zero air before sampling. In order to inspect the cleanliness

149    and vacuum in canisters, the pre-cleaned canisters, after storing for 24h, were analyzed using

150    GC-MS according to the same analytical procedures used to analyze the field samples. The

Atmospheric
Chemistry
and Physics
Discussions

151 canisters without any contamination were used for sampling. No obvious emission source was

152 present during the sampling events. Daily calibration was performed using 2 ppbv standard

153 mixtures to ensure the consistency and sensitivity of GC-MSD/FID system. The deviation in

154 standard values was within ±20%. Abnormal QA/QC data with extremely high or low responses

155 was recalibrated until the deviation was within the acceptable range.

**2.4 Positive matrix factorization (PMF)**

156

157 U.S. EPA PMF 5.0 was used for source apportionment (Liu et al., 2008b;Lau et al.,

158 2010;Abeleira et al., 2017;Xue et al., 2017). Paatero and Tapper (1994) and Paatero (1997)

159 thoroughly illustrated the rationale of PMF. Briefly speaking, PMF is a diagnostic method

160 involving multivariate analysis, and involves decomposing the integrate sample data into two

161 matrices, namely the source profiles and the source contributions. The method takes advantage of

162 other observation data, such as wind direction and speed. The analyst could get messages on major

163 emission sources, which contribute to ambient VOCs. Detailed information on the application of

164 PMF can be referred to the publications cited above and to the PMF 5.0 user manual (U.S. EPA,

165 2014).

166 Based on the chemical mass balance between the input concentrations and the chemical

167 profiles, PMF regarded the ambient data $x_{ij}$, namely the concentration of $j^{th}$ constituent in $i^{th}$ sample,

168 as the gross values contributed by $p$ sources according to Eq. (1).

169
$$X_{ij} = \sum_{k=1}^{p} g_{ik} f_{kj} + e_{ij} \qquad (1)$$

170 where $g_{ik}$ stands for the contribution of $k^{th}$ factor in the $i^{th}$ sample , while $f_{kj}$ is the load of $j^{th}$

171 compound in the $k^{th}$ source. Furthermore, $e_{ij}$ is the relevant residual.

172 In order to avoid negative source contributions, penalty function was adopted for constraints.

173 Each data point can be individually weighed in the model, while the samples with lots of missing

174 values were excluded.

175    Based on the algorithm on uncertainties (U), expressed as $Q$ values, the stability of running

176    results was assessed according to Eq. (2).

177
$$Q = \sum_{i=1}^{n} \sum_{j=1}^{m} \left[ \frac{x_{ij} - \sum_{k=1}^{p} g_{ik} f_{kj}}{u_{ij}} \right]^2 \quad (2)$$

178    where $u_{ij}$ stands for the uncertainty of the $j^{th}$ compound in $i^{th}$ sample.

179    In the PMF model, uncertainty is a function to evaluate the deviations in sampling and analysis

180    procedure (Paatero, 2007). The uncertainty (U) can be calculated based on Eq. (3) (Polissar et al.,

181    1998).

182
183
$$U = \begin{cases} \sqrt{\left(EF \times concentration\right)^2 + \left(MDL\right)^2} & (conc.>MDL) \\ \frac{5}{6} MDL & (conc. \leq MDL) \end{cases} \quad (3)$$

184    where $EF$ signifies the error fraction that equals 100 times of the percentage uncertainty.

185    **3 Results and discussion**

186    **3.1 Mixing ratios and meteorological variations**

187    The total concentrations of PAMS ($\Sigma_{PAMS}$) were different for all four sites (Table 2), and the

188    ranks were inconsistent between each sampling month. In May 2017, the highest $\Sigma_{PAMS}$ was

189    reported at JK (37.65$\pm$22.58 ppbv), followed by GS (31.73$\pm$18.70 ppbv), YH (30.05$\pm$16.43

190    ppbv) and MEM (29.05$\pm$15.34 ppbv), while the $\Sigma_{PAMS}$ values for the month of June, July, August

191    and September were found to be in the order of: GS>JK>MEM>YH, MEM>GS>JK>YH,

192    YH>MEM>JK>GS, and MEM> YH > GS >JK, respectively. Beside the emission sources (to be

193    discussed in Section 3.2), the meteorological conditions also contributed to the variations. For

194    instance, the prevailing wind in May was northwestern at MEM, GS and YH, while the

195    southwestern wind was dominant at JK. The transportation of air pollutants from urban center and

196    industrial plants meant that the highest level of $\Sigma_{PAMS}$ was seen at JK. In June 2017, the prevailing

197    wind vector changed to southeastern at MEM and GS. The average wind speed at GS (0.74$\pm$0.33

198    m s$^{-1}$) was significantly lower than that at MEM (1.84$\pm$0.94 m·s$^{-1}$), indicating poor dispersion

199    conditions at GS. Furthermore, the air pollutants emitted from MEM were more accumulated at GS,

200    which was due to higher $\Sigma_{PAMS}$ at GS ($39.29 \pm 25.37$ ppbv) than that at MEM ($30.28 \pm 12.77$ ppbv).

201    It should also be noted that, when $\Sigma_{PAMS}$ at JK was higher than that of GS, the levels at YH were

202    higher than those of MEM, and vice versa. ~~Based on their geographic locations, both the GS and~~

203    ~~MEM were located in the western part of Zhengzhou city, while JK and YH were situated in the~~

204    ~~eastern side of the city.~~ Except for the discriminations between the pollution sources at every site,

205    the above phenomenon might be a result of topographical effect.

206         $C_2$ - $C_5$ alkanes, acetylene, ethylene, toluene and benzene were the most abundant PAMS

207    detected at all sites (Table 3). These chemicals ~~had the~~ contribution of >60% for $\Sigma_{PAMS}$,

208    representing the general consistency of pollution sources in the region. The mixing ratios of toluene

209    varied within a wide range at each site. Toluene is an important aromatic and has a variety of

210    emission sources (Wang et al., 2014;Barletta et al., 2005), among which, ~~the~~ vehicle exhaust and

211    solvent usage are the major contributors. Due to variable origins and emission strengths, few

212    compounds exhibited wide ranges in certain months. The mixing ratios of cyclohexane, isopentane,

213    toluene, and isobutane had large deviations at MEM in June, which were attributed to the increase

214    in liquefied petroleum gas (LPG) and gasoline evaporation due to the increase in ambient

215    temperatures (Li et al., 2017a;Liu et al., 2008a). At YH and GS, the largest deviations were seen in

216    the month of September. The mixing ratios of fossil fuel combustion markers, such as acetylene

217    ($5.08 \pm 8.36$ ppbv), toluene ($4.37 \pm 5.28$ ppbv), and m,p-xylene ($1.09 \pm 1.62$ ppbv) were varied

218    significantly at YH (Zheng et al., 2017). The variations in propane ($10.77 \pm 17.73$ ppbv), n-butane

219    ($7.55 \pm 13.79$ ppbv), isobutane ($5.46 \pm 10.76$ ppbv) and isopentane ($5.25 \pm 8.76$ ppbv) at GS were

220    reasonably significant due to the evaporation of gasoline and the use of LPG (Li et al., 2017a;Liu et

221    al., 2008a). Both cases demonstrate the widespread combustion sources and fuel evaporation in

222    Zhengzhou city.

223         Among these organic classes, alkane was the most abundant (Fig.2), and accounted for

224    52.85%, 62.52%, 53.38%, 53.39% of the total $\Sigma_{PAMS}$ values at JK, MEM, GS, and YH, respectively.

225    The highest composition of alkane was observed at MEM due to the stronger contributions of

226    ethane, iso-pentane and other branched alkanes (such as, the ones having carbon number of 7 - 8).

Atmospheric
Chemistry
and Physics
Discussions

227    Wang et al. (2017b) reported that these compounds could originate from the cooking process,

228    which is consistent with the results reported here, as there was a shopping mall with a number of

229    canteens around 200 m northeast to the sampling station. In addition, many restaurants were also

230    scattered around.

231        In comparison, the aromatic compounds showed lower compositions in the afternoons (for

232    example, around 14:00 LT) than the mornings (for example, around 07:00 LT) (Fig. 2). Increases in

233    alkene compositions were mainly ascribed to higher contributions of isoprene, which was emitted

234    from biogenic sources at higher temperature and solar irradiation. Isoprene's contribution to $\Sigma_{PAMS}$

235    value at JK at was 12% at 14:00 LT (Fig.2), which was much higher than the other three sites.

236    These results are in accordance with its larger vegetation coverage in the surrounding areas.

237        The average $\Sigma_{PAMS}$ values in Zhengzhou city was significantly lower than those in Beijing

238    (65.55 ppbv), Hangzhou (55.9 ppbv), Guangzhou (47.3 ppbv) and Nanjing (43.5 ppbv), though they

239    were higher than that in Wuhan (23.3±0.5ppbv) (Guo et al., 2012;Li and Wang, 2012;An et al.,

240    2014;Lyu et al., 2016;Raysoni et al., 2017). Furthermore, population density, industrial activity,

241    fuel composition, local stringent regulations for environmental protection, terrain, and weather

242    contributed to their abundances. Alkanes were generally the largest contributor in most areas (Fig.

243    2), while the compositions of aromatics were relatively lower in Zhengzhou city. It is well known

244    that aromatics mainly originate from solvent usage and vehicle exhaust. It is also worth mentioning

245    that Zhengzhou has less manufacturer involved in shoemaking and shipbuilding than Guangzhou

246    and Nanjing. The registered number of vehicles was also lower than that in Beijing. On the other

247    hand, higher composition of alkyne was observed in Zhengzhou. Alkyne typically originates from

248    combustion sources. Henan is the largest agricultural province in China. As the sampling duration

249    covered the crop harvest in June, the residents often used crop residues as the biofuel for their

250    subsistence, thus resulting in higher alkyne compositions.

251    **3.2 Temporal variations**

252        The time series of mixing ratios of CO, SO$_2$, NO, NO$_2$, O$_3$ and PAMS at every site are shown

253    in Fig. 3. Both the *T* and *RH* are also included in Fig. 3. The results showed that there is a

254    distinctive temporal characteristic, during which, lower levels of all air pollutants were observed in

255    July and August (mid-summer) than in other months. These results were similar to those obtained

256    for other urban areas (Li and Wang, 2012;Cheng et al., 1997;Na et al., 2001). Changes in boundary

257    layer depth, human activities, and abundance of hydroxyl radicals (•OH) were the potential causes

258    for the phenomenon. Pal et al.(2012) reported that the height of atmospheric boundary layer was

259    positively correlated with temperature. ~~In the current study, the highest ambient temperature was~~

260    ~~observed in July, while t~~he occurrence of precipitation was more frequent in most areas of China

261    during ~~this period. Furthermore, stronger dispersion efficiently offered a~~ wash-out ~~effect for~~

262    ~~diluting the~~ air pollutants ~~to lower levels in~~ ambient air. Additionally, a series of effective local

263    policies, such as prohibition of painting and coating in open air and limitations on fuel supply

264    between 10:00 -17:00 LT during hot summer days assisted in suppressing the ~~VOCs'~~ emissions.

265    Meanwhile, many organizations, such as schools, institutes and scattered private workshops, were

266    closed due to summer vacations. Some large-scale industries also stopped manufacturing processes

267    for two weeks during this period. Due to this, the anthropogenic emissions reduced, which in turn

268    resulted in a decrease in VOCs, $SO_2$, and $NO_x$ emissions. The reduction of precursor levels and

269    unfavorable photochemical conditions (such as, higher RH and WS) resulted in the $O_3$ levels to be

270    constantly below the standard.

271        As demonstrated in Fig. 3, the observed $\Sigma_{PAMS}$ values at 07:00 LT were often higher than those

272    at 14:00 LT. The accumulation of pollutants during night-time and the temperature inversion in the

273    morning were the most reasonable explanations for this phenomenon. Stronger photochemical

274    reaction during noon-time led to the reduction in atmospheric VOCs. It should be noted that

275    pronounced $\Sigma_{PAMS}$ were occasionally observed at MEM and GS, which were potentially ascribed to

276    sharp changes in local emissions and meteorological conditions. At MEM, the distinctive increment

277    was always accompanied by obvious uplift of alkanes or aromatics. Combined with the changes in

278    other parameters, such as levels of NO, $NO_2$, $SO_2$, CO, RH and T, it was concluded that the

279    abnormally high $\Sigma_{PAMS}$ values at MEM were mainly caused by enhanced combustion sources. Due

280    to the disturbance from solvent use for building renovation, extremely high levels of aromatics

281    were observed at GS in June. In addition, there were potential impacts from gas-fueled power

Atmospheric
Chemistry
and Physics
Discussions

282    plants, which were located about 1 km northwest of the site. Compressed natural gas (CNG) or

283    LPG consumptions resulted in an increase in mixing ratio of propane, isobutane and n-butane

284    (Huang et al., 2015b), which was found consistent with the observations at this site.

285    Acetylene is a stable chemical compound that mainly originates from the combustion of

286    biomass/fossil fuel. On the morning of 5$^{th}$ September (highlighted in pink in Fig. 3), alkyne was

287    found in extremely high concentrations (14.65 - 39.42 ppbv). Its mixing ratio in most of the urban

288    areas was <10 ppbv (Louie et al., 2013;Duan et al., 2008;Guo et al., 2012). It was learnt that the 5$^{th}$

289    September is a festival day for the people, who worship their ancestors. A large number of incenses

290    and offerings, made up of wood and paper, were burnt during the festival, resulting in an increase in

291    the mixing ratio of acetylene all over the Zhengzhou city.

292    **3.3 Spatial variations**

293    Average $\Sigma_{PAMS}$ were higher at industrially impacted sites of GS (31.66±28.73 ppbv) and JK

294    (28.63±22.04 ppbv) than those at the other two sites (MEM and YH). Additionally, the air

295    pollutants related to the combustion process, such as $SO_2$ and CO were also in abundance in

296    western area of Zhengzhou (GS and MEM), where stronger emission sources were related to the

297    combustion of biomass or fossil fuel. Meanwhile, the $O_3$ levels did not present the same trend with

298    $\Sigma_{PAMS}$ among the four sites, indicating that the transformation between $O_3$-$NO_x$-VOCs was more

299    complex than the linear reactions.

300    In June, the $O_3$ concentration often exceeded the national standard level of 80 ppbv. The

301    average mixing ratio of $O_3$ during daytime (07:00-18:00 LT) at JK, MEM, YH, and GS were 74.87

302    ±39.55 ppbv, 73.50±40.59 ppbv, 73.81±35.69 ppbv, and 87.99±46.11 ppbv, respectively. The

303    order of these values is consistent with that of the $\Sigma_{PAMS}$, in which the higher levels were observed

304    at JK and GS. Combined with the higher solvent usages, highest aromatics levels and the severer $O_3$

305    pollutions were found at GS as expected. Even though both the $\Sigma_{PAMS}$ and higher $O_3$ formation

306    potential compounds (such as, alkenes and aromatics) at MEM were a bit higher than those at YH,

307    a reverse order of $O_3$ concentration was observed. Such phenomenon could be attributed to other

308    critical precursors, such as $NO_x$, which are involved in the formation of $O_3$. NO at MEM (8.48±

309     25.74 ppbv) was significantly higher than that at YH ($2.57 \pm 3.08$ ppbv) during daytime, indicating

310     that the reaction between $O_3$ and NO was more efficient at MEM.

311        It is well known that $O_3$ pollution is a regional problem. Streets et al. (2007) reported that the

312     contribution of air pollutants, derived from Hebei, was around 35 - 60% to the pollution in Beijing,

313     which experienced $O_3$ episodes. Along with the decrease in ambient temperature and light intensity,

314     and an increase in RH, the number of non-attainment $O_3$ days theoretically reduced after June, 2017,

315     while the maximum was observed on August 10th, 2017 (highlighted in yellow in Fig. 3). VOCs are

316     the critical contributors to the formation of $O_3$. The reductions in $\Sigma_{PAMS}$ in the afternoons (around

317     14:00 LT) compared to mornings (around 07:00 LT) may have originated from the uptake by $O_3$

318     formation (Fig. 4). Furthermore, the highest VOCs concentration was observed at YH, which was

319     due to its downwind position to the other three sites between 08:00 - 15:00 LT on August 10th (Fig.

320     4). Additionally, the transmission of pollutants led to an abnormally high $O_3$ level at YH.

321        Overall, when the synoptic conditions, such as *T*, *RH* and *WS* were favorable, the $O_3$ level was

322     accompanied by the increase in VOCs concentrations, which potentially demonstrated that the $O_3$

323     formation was more sensitive to the abundance of VOCs in Zhengzhou city.

324     **3.4 Ratios of specific compounds**

325        Ratios of specific VOCs are useful indicators to identify the emission sources (Raysoni et al.,

326     2017;Liu et al., 2015;Li et al., 2017c;Huang et al., 2017;Ho et al., 2009). In order to characterize

327     the differences in the contribution of various sources at each site, two ratios of toluene/benzene and

328     i-pentane/n-pentane were discussed. The ratio of toluene to benzene (T/B) is an efficient tool to

329     differentiate between pollution sources, such as vehicle exhaust, coal combustion and solvent use

330     (Sun et al., 2018). As shown in Fig. 5, the T/B ratio showed variation during days and months. In

331     addition, the correlations between toluene and benzene were different throughout the sampling

332     period, indicating that their emission sources were always changing. The atmospheric lifetimes for

333     toluene and benzene are 1.9 days and 9.4 days, respectively, while the abundance of •OH was

334     assumed to be $10^6$ rad cm$^{-3}$ (Monod et al., 2001). Therefore, toluene was consumed more rapidly

335     than benzene during the photochemical reaction. Due to this reason, the T/B ratios at 14:00 LT

336    were almost lower than those at 07:00 LT. However, in September, higher T/B ratios at 14:00 LT

337    were observed more frequently at MEM and YH than the other station. Meanwhile, the values were

338    increased regionally, which was in accordance with the weaker photochemical reactions in late

339    summer.

340        The $R^2$ value for the correlation between benzene and toluene was better in May (0.73 - 0.84)

341    than during other months for all sites, and the average ratio in this month varied within the range of

342    1.81 - 3.36 for all four sites. Both the tunnel studies and roadside researches indicated that T/B ratio

343    varied within the range of 1 - 2 when the atmosphere was heavily impacted by vehicle emissions

344    (Gentner et al., 2013;Tang et al., 2007;Huang et al., 2015b;Wang et al., 2002). When the ratio was

345    less than 0.6, it may be due to other sources, such as coal combustion and biomass burning (Tsai et

346    al., 2003;Akagi et al., 2011). The industrial activity becomes more important when the value of T/B

347    ratio is higher than 3 (Zhang et al., 2015). The results suggest that evident impacts were observed

348    from vehicle emissions on the T/B ratio during the sampling period. Except for September, the

349    average T/B ratio at JK lied within the range of 1.47 - 2.72, which was due to the vehicle emissions.

350    Due to less interruption from photochemical reaction, the impact from industrial activities, which

351    were mainly related to industrial clusters composed of automotive–related workshops and printing

352    shops, and located approximately 2 km southwest of the observation site became important and

353    resulted in higher T/B value (3.89) in September at JK. It is apparent that the T/B ratio at MEM was

354    on the low side during the period of May - August (0.96 - 1.68), highlighting the impact of

355    coal-fired thermal power plant. After excluding the abnormal values, the average ratio at GS (0.44 -

356    1.17) exhibited clear characteristics related to the combustion of coal/biomass during the period of

357    June - August. This was related to the fact that the region was located on the edge of Zhengzhou.

358    The impacts from biomass burning would be heavier than in other areas during the harvesting

359    season. On the other hand, the coal fired power plant next to SZ was located at the southeast of GS

360    with the linear distance of 5 km between the two points. Considering that the prevalent wind

361    direction was southeastern during the period of June - August, the air pollutants emitted from the

362    power plant could be easily transported to this region. Overall, the emission sources related to

363    industrial activities were more evident in September. It is likely that the traffic emissions at JK and

Atmospheric
Chemistry
and Physics
Discussions

364    combustion sources related to coal or biomass at MEM and GS would account for more

365    contributions to VOCs, while there were no consistent results observed for YH due to the wide span

366    of T/B ratio (1.07 - 5.38).

367    i-Pentane has similar reactivity to n-pentane (Jobson et al., 1998). The ratio between these two

368    VOCs is useful in differentiating the potential sources, such as natural gas drilling and vehicle

369    emissions. In this study, i-pentane and n-pentane were highly correlated ($R^2$=0.78 - 0.89)

370    throughout the whole sampling campaign (Fig. 6), indicating stable sources for these two

371    compounds. In the area, heavily impacted by natural gas drilling, the ratios lied within the range of

372    0.82 - 0.89 (Gilman et al., 2013;Abeleira et al., 2017). Higher values were often reported for

373    automobiles, such as 2.2 - 3.8 for vehicle emissions, 1.8 - 4.6 for fuel evaporation, and 1.5 - 3.0 for

374    gasoline (Russo et al., 2010;McGaughey et al., 2004;Jobson et al., 2004;Wang et al., 2013b). Low

375    values within the range of 0.56 - 0.80 were found for coal combustion. The highest ratio was

376    observed at JK (2.73), which was comparable to the value of 2.93 reported in a Pearl River Tunnel

377    (Liu et al., 2008a), thus indicating strong impacts from traffic-related sources. The average ratio at

378    MEM (2.02) was inconsistent with the characteristics of coal combustion. Yan et al. (2017)

379    reported that the ratio for areas, which include several coal-fired thermal power plants, was

380    approximately 0.55. The variation could be explained by factors, such as production scales, fuel

381    compositions, sampling time and terrain. Additionally, it is remarkable that MEM was surrounded

382    by a main road with four traffic lanes. The distance between the nearest traffic light and the

383    sampling site was just 200 m. Frequent idling may cover up the contribution from coal combustion,

384    thus overshadowing the effect of traffic emissions. The average ratio at GS (1.85) was close to that

385    at YH (1.68). This was due to the similarity between the traffic related sources (such as, gasoline

386    and fuel evaporation). The results showed that the vehicle emissions were an important source for

387    VOCs in Zhengzhou city.

388    **3.5 Reactive chemicals**

389    Due to large differences in the reactivity of individual species, the contribution of each

390    component to $O_3$ formation was different. Ozone formation potential (OFP) is a useful tool to

Atmospheric
Chemistry
and Physics
Discussions

391  identify local active species that contribute the most to $O_3$ pollution (Huang et al., 2017). OFP is

392  calculated using Eq. (4).

393  $$OFP = C_i \times MIR \qquad (4)$$

394  where $C_i$ represents the concentration level of $i^{th}$ species, while $MIR$ is a constant taken from Carter

395  (2010) (Table 1).

396  Different from the results reported by (Wu and Xie, 2017), based on the emission inventory for

397  North China Plain (NCP), YRD and PRD, where the largest contributor was the aromatics,

398  followed by alkenes, alkenes were the most significant contributors ($55.91 \pm 14.17\%$) to the sum of

399  OFP in Zhengzhou city. The biggest contributors included ethylene, isoprene, m,p-xylene, toluene,

400  propylene, acetylene, n-butane, i-pentane and propane, and their contributions lied within the range

401  of 74.64 - 79.90% of the sum of OFP (Table 5). The composition of acetylene was higher compared

402  to other areas (Li and Wang, 2012;Jia et al., 2016), demonstrating that it is necessary to conduct

403  emission controls on sources related to combustion in Zhengzhou city.

404  It is well known that the ratio between VOCs and $NO_x$ is an important index to analyze

405  variable $O_3$ concentrations (Toro et al., 2006;Simon et al., 2015;Geng et al., 2009;Jin and Holloway,

406  2015;Geddes et al., 2009;Li et al., 2017b). Zhengzhou suffered from the severest $O_3$ pollution in

407  June, 2017. The relationships between OFP of each organic group, $\Sigma_{PAMS}$, and the concentrations of

408  $NO_x$ and $O_3$, as well as the corresponding meteorological conditions, are shown in Fig. 7. At every

409  site at 07:00 LT, WS was generally lower than that at 14:00 LT, indicating weaker vertical

410  distribution. With the lower RH and higher T and OFP ($88.13 \pm 30.32$ ppbv) values, lower $O_3$ was

411  unexpectedly seen at YH than MEM on sunny days, which was attributed to lower $\Sigma_{PAMS}/NO_x$

412  ratios at YH (highlighted in pink in Fig. 6). The total OFP was higher at JK than at other sites,

413  although the actual $O_3$ levels at JK were very close to those at MEM and even lower than those at

414  GS. A lower WS at GS ($0.65 \pm 0.26$ m s$^{-1}$) promoted the pollutant accumalation The ratio of

415  $\Sigma_{PAMS}/NO_x$ was more scattered at JK and MEM than at YH and GS along with the variable WS,

416  thus demonstrating significant impacts from metelogical conditions. During clear days, higher $O_3$

Atmospheric
Chemistry
and Physics
Discussions
Open Access
EGU

417  concentration was always accompanied by higher $\Sigma_{PAMS}/NO_x$ ratio at each site, indicating a close

418  relationship between the $\Sigma_{PAMS}/NO_x$ ratio and $O_3$.

### 3.6 Source apportionment

420  In order to select appropriate chemical species for PMF model, following principles were used.

421  Species with mixing ratios usually below MDL were eliminated. Except for the source markers,

422  species with high reactivity should be excluded (Shao et al., 2016;Guo et al., 2011). Finally, 28

423  VOC species and $NO_2$ were chosen for the source analysis. Q(robust), Q(true) and Q(true)/Q(exp)

424  are presented in Table 6. Based on the model results, seven factors were defined at MEM, YH, and

425  GS, while eight factors were defined at JK (Fig.8).

426  Source profiles showed that the sites had similar regional characteristic. There was a strong

427  common source (factor 1) for $C_2$ - $C_5$ n-alkanes and certain amounts of $C_2$ - $C_4$ alkenes, benzene,

428  toluene, acetylene and $NO_2$.It is reported that i-Pentane and aromatics (such as, benzene, toluene,

429  ethylbenzene and m/p-xylene) usually originated from gasoline evaporation, while isobutane and

430  n-butane were emitted from LPG/CNG usage (Li et al., 2017a;Liu et al., 2008a). Considering the

431  wide consumption of CNG for residential cooking in Zhengzhou, this factor was defined as

432  CNG+gasoline evaporation.

433  The second factor was characterized based upon significant loading of toluene, ethylbenzene,

434  m/p-xylene, and 1,2,4-trimethylbenzene. According to previous studies (Yuan et al., 2010;Wang et

435  al., 2014), toluene and $C_8$ - $C_9$ aromatics were the major VOCs emitted from paint applications.

436  Therefore, Source 2 was assigned as the solvent use. This is consistent with the real situation that

437  there were widespread road paving and building constructions in Zhengzhou city. In addition, car

438  decoration, printing, and furniture manufacturing, which are associated with the use of adhesives,

439  were also included in this source category.

440  The third source was associated with the significant portion of long chain alkanes ($C_7$ - $C_9$) and

441  high amounts of toluene, which are tracers for diesel evaporation (Liu et al., 2008a). Therefore,

442  Source 3 was identified as the diesel vapor. Beside on-road vehicles, many non-road mobile

443  machineries used for building or railway station constructions were correlated with this source.

444    Source 4 was dominated by trans-2-butene and 1-butene. These species were mainly produced

445    in coal combustion (Liu et al., 2008a;Yan et al., 2016). Liu et al. (2016b) reported that 1-butene

446    was a critical VOC generated during the smoldering process of coal combustion. This factor was

447    thus categorized as the coal combustion.

448    The fifth factor shows a dominant loading of cyclohexane, methylcyclohexane, styrene,

449    2-methylhexane and 3-methylhexane. The first three VOCs were identified as the components

450    heavily impacted by petrochemical industries (Jobson et al., 2004). Therefore, this source was

451    defined as the petrochemical.

452    Source 6 was composed of ethylene, propylene, benzene, toluene, 3-methylpentane, n-heptane,

453    acetylene and $NO_2$. In urban areas, vehicle emissions are a major source for ethylene and propylene

454    (Wang et al., 2017a). Fossil fuel combustion produces large amounts of acetylene (Ho et al., 2009),

455    while $NO_2$ is a typical tracer for vehicle exhaust (Huang et al., 2015a). The source was referred to

456    as the vehicle exhaust.

457    Source 7 was distinguished by extremely high compositions of isoprene, a species mainly

458    produced by vegetation through photosynthesis (Millet et al., 2016). Even though, it can be emitted

459    from traffic-related sources (Yuan et al., 2009), this possibility can be ignored by its poor

460    correlations with other source makers of vehicle exhaust (such as, i-pentane and ethylene).

461    Therefore, this source was identified as the biogenic emissions.

462    Factor 8 was only resolved for the JK site. The major compounds present in this source were

463    ethylene, propylene, acetylene and $NO_2$. These compounds mainly originated from on-road vehicles

464    (Wang et al., 2017a). Since there were minor contributions of alkanes and aromatics, they were

465    possibly derived from on-road vehicles under different running conditions. This factor was named

466    as the traffic-related source.

467    According to the source apportionment results (Fig. 9), CNG usage, gasoline evaporation and

468    vehicle exhaust had considerable portions and were the important sources for ambient VOCs at

469    every site. The smallest contribution from CNG and gasoline evaporations was found at GS

470    (24.99%), which was lower than the values observed at JK (35.06%) and YH (34.28%), and was

471      probably caused by the heavier traffic at JK and larger consumption of CNG (from the condensed

472      canteens and active household cooking) at YH. The distribution of petrochemical source was

473      uneven on the regional scale, with the largest portion observed at MEM (11.56%) and comparable

474      values found for JK (3.44%), YH (6.21%) and GS (5.56%). These results are in accordance with

475      the fact the distance between the petrochemical plants and the sampling site of MEM was the

476      shortest (*ca*. 2 km). The weighted percentages attributed to the solvent use were similar among the

477      four sites, with the highest value of 12.41% at MEM, which was consistent with the fact that there

478      was less abundance of aromatics in Zhengzhou city. The emission source related to diesel fuel was

479      more evident at JK (11.76%). The area was rife with logistics companies and frequently suffered

480      from disturbance of heavy-duty cargo vehicles powered by diesel fuel. Coal combustion impacted

481      the ambient air heavily at MEM (17.84%) and GS (13.50%), which were only 2 km and 5 km away

482      from the thermal power plants, respectively. Overall, the traffic-related source was the most

483      important emission source for VOCs in Zhengzhou, which is in accordance with the results

484      obtained for other urban areas (Yuan et al., 2013b;Lyu et al., 2016;Lau et al., 2010).

485      **3.7 Long-range transport**

486      Air transported from surrounding areas had impacts on the air quality at the study site

487      (Langford et al., 2010;Sun et al., 2018). In this work, Hybrid Single-Particle Lagrangian Integrated

488      Trajectory (HYSPLIT) model was used to present the long-range transport effects on the air quality

489      of Zhengzhou city (Fig. 10). Meteorological conditions are important factors that impact both the

490      compositions and levels of VOCs. Clusters arriving at Zhengzhou in May, 2017 demonstrated

491      longer paths, and included six clusters in total. The largest ~~one~~ (27.2%) was originated from

492      Yinchuan city, which is a central city in northwest China. The cluster passed over several

493      non-capital cities (such as, Yanan, Yuncheng and Luoyang) in Shanxi and Sichuan provinces. Such

494      long-range transportation of pollutants might have less impact on the air quality of Zhengzhou,

495      which agrees well with the comparable levels and similar compositions of VOCs during the period

496      of May - June. In the months of June, August and September, approximately half of the air currents

497      originated from the areas of Henan province. The air current originating from Hubei province took

498      up the largest portion (*ca*. 88.68%) of clusters in July, and potentially led to a significant variation

Atmospheric
Chemistry
and Physics
Discussions

499    in the concentration or composition of VOCs. As illustrated in Fig. 2, the average concentration

500    level of $\Sigma_{PAMS}$ in July sharply decreased to 15.91±6.54 ppbv. This was accompanied by the

501    weighted percentage of aromatics, which dropped to 10.30±4.23%. It is well known that alkenes

502    and aromatics have high photochemical reactivity. The T/B ratio also showed the lowest level

503    (1.15±0.99) around this period, illustrating that the air plumes had longer lifetime. Both of these

504    evidenced that Zhengzhou was impacted by air pollutants, which originated from Hubei province.

505    According to previous studies in Wuhan, the capital city of Hubei province, the average total $\Sigma_{PAMS}$

506    (23.3±0.6 ppbv) (Lyu et al., 2016) was much lower than the average level in Zhengzhou

507    (31.57±23.35 ppbv). The cleaner air mass clusters, originating from Hubei in July, can thus be

508    designated as a dilute flow.

509    **4. Conclusions**

510       In this study, PAMS were collected at four different sites in Zhengzhou, Henan (China) for the

511    first time. $C_2$ - $C_5$ alkanes, acetylene, ethylene, toluene and benzene were the most abundant VOCs

512    in the region. On the basis of monthly average, the maximum $\Sigma_{PAMS}$ was observed at GS, which

513    was impacted by various emission sources. In comparison to other Chinese cities, the weighted

514    percentage of aromatics was lower, while higher alkyne level was observed in Zhengzhou city. Due

515    to less anthropogenic emissions and more favorable dispersion conditions, most of the air pollutants

516    had the lowest levels in the mid-summer month of July. Overall, the $O_3$ levels were correlated with

517    $\Sigma_{PAMS}$, which potentially demonstrated that the $O_3$ formation was more sensitive to the abundance

518    of VOCs in Zhengzhou. Different from other megacities, alkenes were the biggest contributors to

519    OFP, while acetylene was particularly critical at each site. The CNG usage, gasoline evaporation

520    and vehicle exhaust were the important sources for ambient VOCs. Cleaner air clusters from Hubei

521    occasionally arrived at Zhengzhou. This study provides the first-hand information on the

522    characteristics of VOCs and assists in overcoming the $O_3$ pollution issue in Zhengzhou city, China.

526

Atmospheric
Chemistry
and Physics
Discussions

Open Access

527  **Table & Figure**

528            Table1. Detailed information on the calibration curve for 57 PAMS and their MIR

| | Species | $R^2$ | MDL(pptv) | RSD | MIR | | Species | $R^2$ | MDL(pptv) | RSD | MIR |
|---|---|---|---|---|---|---|---|---|---|---|---|
| | Ethane | 0.9998 | 6.8 | 5% | 0.28 | | Ethylene | 0.9997 | 12.5 | 10% | 9 |
| | Propane | 0.9998 | 2.8 | 2% | 0.49 | | Propylene | 0.9998 | 6.2 | 5% | 11.66 |
| | Isobutane | 0.9998 | 3.2 | 3% | 1.23 | | Trans-2-butene | 1 | 3.6 | 6% | 15.16 |
| | n-Butane | 0.9998 | 6.7 | 5% | 1.15 | | 1-Butene | 0.9995 | 7.8 | 6% | 9.73 |
| | Cyclopentane | 0.9971 | 8.5 | 7% | 0.09 | | Cis-2-butene | 0.9997 | 6.8 | 6% | 14.24 |
| | Isopentane | 0.9999 | 5.5 | 4% | 0.93 | **Alkene** | 1,3-butadiene | 0.9874 | 13.5 | 8% | |
| | n-Pentane | 0.9999 | 6.6 | 5% | 0.88 | | 1-Pentene | 0.9764 | 6.3 | 5% | 7.21 |
| | 2,2-Dimethyl-butane | 0.9963 | 5.4 | 4% | 1.17 | | Trans-2-pentene | 0.9964 | 10.1 | 7% | 10.56 |
| | 2,3-Dimethylbutane | 0.9966 | 7.6 | 6% | 0.97 | | Isoprene | 0.9966 | 7.7 | 6% | 10.61 |
| | 2-Methylpentane | 0.9958 | 8.0 | 6% | 1.5 | | Cis-2-pentene | 0.9965 | 8.6 | 7% | 10.38 |
| | 3-Methylpentane | 0.9967 | 5.4 | 4% | 1.8 | | 1-Hexene | 0.9961 | 11.4 | 9% | 4.4 |
| **Alkane** | n-Hexane | 0.9967 | 7.3 | 6% | 1.24 | **Alkyne** | Acetylene | 0.9996 | 7.1 | 5% | 0.95 |
| | 2,4-Dimethylpentane | 0.9972 | 9.6 | 7% | 1.55 | | Benzene | 0.9975 | 6.5 | 5% | 0.72 |
| | Methyl-cyclopentane | 0.9974 | 5.8 | 5% | 2.19 | | Toluene | 0.9963 | 4.3 | 4% | 4 |
| | 2-Methyl-hexane | 0.9968 | 8.6 | 7% | 1.19 | | Ethyl-benzene | 0.9955 | 4.8 | 4% | 3.04 |
| | Cyclohexane | 0.9958 | 7.7 | 6% | 1.25 | | m,p-Xylene[a] | 0.9969 | 12.5 | 5% | 7.8 |
| | 2,3-Dimethyl-pentane | 0.9969 | 6.2 | 5% | 1.34 | | o-Xylene | 0.9954 | 5.2 | 4% | 7.64 |
| | 3-Methyl-hexane | 0.9946 | 8.8 | 7% | 1.61 | **Aromatic** | Styrene | 0.9961 | 10.6 | 8% | 1.73 |
| | 2,2,4-Trimethyl-pentane | 0.9975 | 7.1 | 6% | 1.26 | | Isopropylbenzene | 0.9947 | 4.3 | 4% | 2.52 |
| | n-Heptane | 0.9974 | 9 | 7% | 1.07 | | n-Propylbenzene | 0.9929 | 1.6 | 1% | 2.03 |
| | Methyl-cyclohexane | 0.9972 | 5.8 | 5% | 1.7 | | m-Ethyltoluene | 0.9910 | 7.3 | 6% | 7.39 |
| | 2,3,4-Trimethyl-pentane | 0.9976 | 5.7 | 5% | 1.03 | | p-Ethyltoluene | 0.9994 | 8.4 | 7% | 4.44 |

Atmospheric
Chemistry
and Physics
Discussions

| 2-Methyl-heptane | 0.9971 | 7.0 | 6% | 1.07 | 1,3,5-Trimethyl-benzene | 0.9994 | 6.1 | 5% | 11.76 |
|---|---|---|---|---|---|---|---|---|---|
| 3-Methyl-heptane | 0.9974 | 6.7 | 5% | 1.24 | o-Ethyltoluene | 0.9995 | 4.3 | 4% | 5.59 |
| n-Octane | 0.9973 | 7.6 | 6% | 0.9 | 1,2,4-Trimethylbenzene | 0.9983 | 9.7 | 8% | 8.87 |
| n-Nonane | 0.9963 | 3.4 | 3% | 0.78 | 1,2,3-Trimethylbenzene | 0.9927 | 9.7 | 8% | 11.97 |
| n-Decane | 0.9935 | 7.8 | 6% | 0.68 | m-Diethylbenzene | 0.9967 | 5.2 | 4% | 7.1 |
| n-Undecane | 0.9919 | 7.5 | 6% | 0.61 | p-Diethylbenzene | 0.9950 | 4.2 | 3% | 4.43 |

529    [a] *m*-Xylene and *p*-Xylene are co-eluted in the chromatographic separation.

530

531                          Table 2. Wind speed (m·s$^{-1}$) during the sampling period

|  | JK | MEM | YH | GS |
|---|---|---|---|---|
| **May** | 1.34±0.65 | 1.86±1.19 | 1.27±0.66 | 0.97±0.49 |
| **June** | 1.07±0.48 | 1.86±0.94 | 0.97±0.36 | 0.74±0.33 |
| **July** | 1.48±0.59 | 2.62±1.19 | 1.15±0.45 | 0.90±0.32 |
| **August** | 1.06±0.48 | 1.86±0.94 | 0.95±0.39 | 0.76±0.35 |
| **September** | 0.80±0.38 | 1.24±0.80 | 0.82±0.43 | 0.62±0.38 |

532

533

Atmospheric
Chemistry
and Physics
Discussions

534        Table 3. Concentrations of Top 10 PAMS and $\Sigma_{PAMS}$ (ppbv) at every site during the sampling

535        period

| Site | | JK | | | MEM | | | GS | | | YH | | |
|---|---|---|---|---|---|---|---|---|---|---|---|---|---|
| Item | Species | Mean | Std. | Species | Mean | Std. | Species | Mean | Std. | Species | Mean | Std. |
| | Acetylene | 4.39 | 2.48 | Ethane | 5.17 | 2.18 | Ethane | 4.71 | 2.18 | Acetylene | 4.74 | 2.61 |
| | Ethane | 4.29 | 1.43 | Acetylene | 4.22 | 1.60 | Propane | 3.55 | 3.79 | Ethane | 4.42 | 1.87 |
| | Ethylene | 3.77 | 2.57 | Ethylene | 3.42 | 1.70 | Acetylene | 3.14 | 1.69 | Ethylene | 4.27 | 4.02 |
| | Toluene | 3.19 | 3.36 | Propane | 3.02 | 2.05 | Toluene | 3.05 | 3.66 | Propane | 2.58 | 1.48 |
| | Propane | 2.61 | 1.23 | n-Butane | 1.77 | 1.68 | Ethylene | 2.92 | 1.92 | Toluene | 2.28 | 2.60 |
| May.2017 | Isopentane | 2.52 | 3.03 | Benzene | 1.68 | 2.48 | 2-Methylpentane | 2.56 | 6.54 | n-Butane | 1.54 | 0.95 |
| | n-Butane | 2.20 | 1.75 | Toluene | 1.59 | 1.53 | Isopentane | 1.97 | 1.38 | Isopentane | 1.32 | 1.04 |
| | m,p-Xylene[a] | 2.17 | 2.63 | Isopentane | 1.21 | 0.70 | n-Butane | 1.78 | 1.80 | Isoprene | 1.32 | 1.31 |
| | Benzene | 1.87 | 2.11 | 2-Methylpentane | 1.13 | 2.19 | Cyclohexane | 1.58 | 4.72 | Benzene | 1.19 | 1.07 |
| | Isoprene | 1.75 | 1.67 | Isobutane | 1.13 | 1.33 | Isobutane | 1.52 | 3.14 | Isobutane | 0.84 | 0.53 |
| | $\Sigma_{PAMS}$ | 37.65 | 22.58 | $\Sigma_{PAMS}$ | 29.30 | 15.34 | $\Sigma_{PAMS}$ | 31.73 | 18.70 | $\Sigma_{PAMS}$ | 30.05 | 16.43 |
| | Acetylene | 4.62 | 1.50 | Ethane | 6.33 | 3.09 | Acetylene | 5.03 | 1.83 | Acetylene | 4.60 | 1.41 |
| | Ethane | 3.48 | 1.47 | Cyclohexane | 5.18 | 11.87 | Ethane | 4.49 | 2.52 | Ethane | 3.85 | 1.46 |
| | Ethylene | 3.22 | 1.52 | Isopentane | 4.95 | 8.30 | Ethylene | 3.27 | 1.16 | Ethylene | 3.05 | 0.90 |
| | Propane | 2.32 | 1.43 | Toluene | 4.35 | 8.21 | Toluene | 3.14 | 3.03 | Propane | 2.48 | 0.99 |
| | n-Butane | 2.30 | 2.98 | Isobutane | 4.16 | 10.30 | Ethane | 3.09 | 2.07 | Isoprene | 1.67 | 1.62 |
| June.2017 | Isoprene | 2.08 | 1.58 | Propane | 3.66 | 3.66 | n-Butane | 1.84 | 1.53 | n-Butane | 1.54 | 0.87 |
| | Toluene | 1.99 | 1.79 | Acetylene | 3.45 | 2.05 | m,p-Xylene[a] | 1.83 | 2.75 | Toluene | 1.44 | 1.65 |
| | m,p-Xylene[a] | 1.69 | 2.00 | n-Butane | 2.51 | 3.51 | Isopentane | 1.74 | 1.58 | Isopentane | 1.38 | 1.30 |
| | Isopentane | 1.59 | 1.56 | Benzene | 2.50 | 4.58 | Isobutane | 1.70 | 2.63 | Benzene | 1.04 | 0.61 |
| | Benzene | 1.30 | 0.72 | Ethylene | 2.41 | 1.34 | Benzene | 1.41 | 0.90 | Isobutane | 0.99 | 0.49 |
| | $\Sigma_{PAMS}$ | 34.02 | 19.89 | $\Sigma_{PAMS}$ | 30.28 | 12.77 | $\Sigma_{PAMS}$ | 39.29 | 25.37 | $\Sigma_{PAMS}$ | 28.33 | 11.94 |
| July.2017 | Acetylene | 2.55 | 1.47 | Ethane | 4.00 | 2.08 | Ethane | 2.96 | 1.80 | Ethane | 2.75 | 0.77 |
| | Ethane | 2.30 | 0.95 | Isopentane | 2.13 | 3.84 | Propane | 2.56 | 2.23 | Acetylene | 1.84 | 0.73 |

24

Atmospheric
Chemistry
and Physics
Open Access
Discussions
EGU

|  | | | | | | | | | | | | |
|---|---|---|---|---|---|---|---|---|---|---|---|---|
|  | n-Butane | 1.46 | 0.84 | Acetylene | 2.11 | 0.86 | Isopentane | 1.99 | 2.09 | Isopentane | 1.73 | 2.30 |
|  | Isoprene | 1.42 | 1.45 | Propane | 2.08 | 1.31 | Acetylene | 1.58 | 0.71 | Propane | 1.52 | 0.57 |
|  | Propane | 1.38 | 0.65 | Ethylene | 1.36 | 0.97 | Isobutane | 1.37 | 1.85 | Trans-2-pentene | 1.36 | 1.49 |
|  | Isopentane | 1.26 | 1.24 | n-Butane | 1.36 | 1.12 | n-Butane | 1.36 | 1.12 | n-Butane | 1.08 | 0.55 |
|  | Ethylene | 1.20 | 0.84 | Isobutane | 1.05 | 1.58 | Ethylene | 1.18 | 1.05 | Ethylene | 1.05 | 0.65 |
|  | Isobutane | 0.75 | 0.57 | Toluene | 0.72 | 0.74 | Toluene | 1.15 | 1.81 | Isobutane | 0.98 | 1.22 |
|  | Benzene | 0.51 | 0.22 | Benzene | 0.55 | 0.34 | Isoprene | 1.12 | 0.99 | Toluene | 0.62 | 0.71 |
|  | Toluene | 0.49 | 0.45 | Isoprene | 0.54 | 0.52 | n-Pentane | 0.60 | 0.60 | Benzene | 0.55 | 0.36 |
|  | $\Sigma_{PAMS}$ | 16.01 | 6.13 | $\Sigma_{PAMS}$ | 20.74 | 12.66 | $\Sigma_{PAMS}$ | 19.60 | 13.94 | $\Sigma_{PAMS}$ | 15.95 | 7.54 |
|  | Ethane | 3.41 | 1.62 | Ethane | 5.90 | 2.88 | Ethane | 3.97 | 2.51 | Ethane | 3.77 | 1.43 |
|  | Isopentane | 2.69 | 2.98 | Isopentane | 3.49 | 7.25 | Acetylene | 2.45 | 2.08 | Propane | 2.81 | 1.27 |
|  | Propane | 2.38 | 1.72 | Propane | 2.58 | 1.40 | Propane | 2.12 | 1.33 | Isopentane | 2.58 | 3.93 |
|  | Acetylene | 1.94 | 1.01 | Acetylene | 2.19 | 1.50 | Isopentane | 1.51 | 1.41 | Acetylene | 2.04 | 1.11 |
|  | n-Butane | 1.81 | 1.65 | Ethylene | 1.43 | 0.99 | Ethylene | 1.35 | 1.09 | n-Butane | 1.75 | 0.85 |
| Aug.2017 | Ethylene | 1.52 | 1.28 | n-Butane | 1.41 | 0.90 | Toluene | 1.28 | 1.97 | n-Pentane | 1.72 | 2.63 |
|  | Isoprene | 1.02 | 0.99 | n-Pentane | 1.10 | 1.88 | n-Butane | 1.25 | 0.91 | Toluene | 1.52 | 1.85 |
|  | n-Pentane | 0.98 | 0.89 | Toluene | 0.98 | 1.40 | Isoprene | 0.87 | 0.77 | Ethylene | 1.32 | 0.70 |
|  | Isobutane | 0.90 | 0.71 | Isobutane | 0.91 | 0.76 | n-Pentane | 0.76 | 0.72 | Isobutane | 1.14 | 0.82 |
|  | Toluene | 0.89 | 0.98 | Benzene | 0.53 | 0.28 | Isobutane | 0.68 | 0.47 | Trans-2-pentene | 1.11 | 1.39 |
|  | $\Sigma_{PAMS}$ | 21.54 | 15.29 | $\Sigma_{PAMS}$ | 24.37 | 20.79 | $\Sigma_{PAMS}$ | 20.49 | 15.67 | $\Sigma_{PAMS}$ | 26.03 | 17.01 |
|  | Ethane | 4.66 | 2.21 | Ethane | 6.87 | 3.92 | Propane | 10.77 | 17.73 | Ethane | 5.35 | 2.65 |
|  | Propane | 3.54 | 2.19 | Acetylene | 3.82 | 3.76 | n-Butane | 7.55 | 13.79 | Acetylene | 5.08 | 8.36 |
|  | Acetylene | 3.27 | 3.09 | Isopentane | 3.73 | 6.25 | Isobutane | 5.46 | 10.76 | Toluene | 4.37 | 5.28 |
|  | n-Butane | 2.52 | 1.96 | Propane | 3.31 | 1.83 | Isopentane | 5.25 | 8.76 | Propane | 3.29 | 1.93 |
| Sept.2017 | Ethylene | 2.02 | 1.48 | Toluene | 2.71 | 4.31 | Ethane | 5.08 | 2.20 | Isopentane | 2.89 | 3.02 |
|  | Isopentane | 1.77 | 1.49 | Ethylene | 2.37 | 1.55 | Acetylene | 4.03 | 5.84 | Ethylene | 2.67 | 2.03 |
|  | Toluene | 1.44 | 1.42 | n-Butane | 2.23 | 1.53 | Toluene | 2.50 | 3.54 | n-Butane | 2.47 | 2.19 |
|  | Isobutane | 1.08 | 0.79 | n-Pentane | 1.70 | 2.63 | n-Pentane | 2.33 | 3.44 | n-Pentane | 1.39 | 1.22 |

Atmospheric
Chemistry
and Physics
Discussions

Open Access

| | | | | | | | | | | | |
|---|---|---|---|---|---|---|---|---|---|---|---|
| m,p-Xylene[a] | 0.93 | 1.13 | Isobutane | 1.33 | 1.10 | Ethylene | 2.19 | 1.68 | Isobutane | 1.19 | 0.86 |
| n-Pentane | 0.75 | 0.61 | Benzene | 0.60 | 0.43 | Propylene | 0.73 | 0.76 | m,p-Xylene[a] | 1.09 | 1.62 |
| $\Sigma_{PAMS}$ | 26.20 | 16.22 | $\Sigma_{PAMS}$ | 34.15 | 23.85 | $\Sigma_{PAMS}$ | 30.36 | 19.76 | $\Sigma_{PAMS}$ | 32.56 | 19.76 |

536   [a] *m*-Xylene and *p*-Xylene are co-eluted in the chromatographic separation.

537

Atmospheric
Chemistry
and Physics
Discussions

538

539        Table 4. Average mixing ratios of $NO_x$, $O_3$, CO, $SO_2$ and $\Sigma_{PAMS}$ in the sampling campaign

| Site | NOx | O₃ | CO | SO₂ | ΣPAMS |
|------|-----|-----|-----|-----|-------|
| GS | 32.21±27.24 | 52.53±36.02 | 0.84±0.28 | 6.80±4.33 | 31.66±28.73 |
| JK | 34.11±34.17 | 49.50±33.66 | 0.79±0.31 | 4.51±3.24 | 28.63±22.04 |
| MEM | 36.42±32.21 | 47.09±32.66 | 0.92±0.31 | 6.44±4.75 | 27.67±18.09 |
| YH | 29.31±27.84 | 52.00±31.92 | 0.84±0.25 | 4.95±3.88 | 27.45±18.28 |

540        Note: Units for air pollutants were ppbv except for CO, which was measured in ppmv

541

542        Table 5. Top 10 PAMS ranked according to calculated ozone formation potential (OFP)

| | JK | | | MEM | | | YH | | | GS | | |
|---|---|---|---|---|---|---|---|---|---|---|---|---|
| species | OFP(ppbv) | (%) | species | OFP(ppbv) | (%) | species | OFP(ppbv) | (%) | species | OFP(ppbv) | (%) |
| Ethylene | 18.99 | 25.54 | Ethylene | 18.44 | 30.88 | Ethylene | 19.83 | 28.10 | Ethylene | 18.04 | 25.96 |
| Isoprene | 12.99 | 21.83 | Isoprene | 4.66 | 10.10 | Isoprene | 7.44 | 11.30 | Isoprene | 8.01 | 16.75 |
| m/p-Xylene[a] | 6.08 | 5.89 | Toluene | 3.73 | 6.67 | Toluene | 6.63 | 7.75 | Toluene | 7.43 | 7.67 |
| Toluene | 5.53 | 5.83 | Propylene | 3.60 | 6.16 | m/p-Xylene[a] | 3.93 | 4.38 | Propylene | 4.39 | 5.85 |
| Propylene | 4.03 | 5.36 | Acetylene | 2.82 | 5.00 | Acetylene | 3.15 | 4.38 | m/p-Xylene[a] | 4.31 | 4.57 |
| Acetylene | 2.97 | 4.44 | m/p-Xylene[a] | 2.55 | 4.20 | Propylene | 3.01 | 3.60 | Acetylene | 2.76 | 4.24 |
| n-Butane | 2.15 | 3.05 | n-Butane | 1.81 | 3.20 | Trans-2-pentene | 2.25 | 2.94 | n-Butane | 1.82 | 2.93 |
| o-Xylene | 1.83 | 2.00 | Isopentane | 1.76 | 3.16 | n-Butane | 1.84 | 2.80 | Isopentane | 1.71 | 2.68 |
| Isopentane | 1.66 | 1.95 | Ethane | 1.58 | 2.96 | Isopentane | 1.59 | 2.22 | Propane | 1.38 | 2.26 |
| Propane | 1.17 | 1.73 | Propane | 1.31 | 2.48 | Propane | 1.18 | 1.98 | Isobutane | 1.13 | 1.98 |

543        [a] *m*-Xylene and *p*-Xylene are co-eluted in the chromatographic separation.

544

545

546 Table 6. Critical parameters for optimizing the PMF results

| Site | JK | | | MEM | | | YH | | | GS | | |
|---|---|---|---|---|---|---|---|---|---|---|---|---|
| Factor Number | 6 | 7 | 8 | 5 | 6 | 7 | 6 | 7 | 8 | 6 | 7 | 8 |
| Q(true) | 2821.61 | 2246.40 | 1859.77 | 2793.06 | 2207.56 | 1789.63 | 2903.47 | 2458.26 | 2025.64 | 3396.21 | 2897.95 | 2520.45 |
| Q(robust) | 2840.41 | 2263.57 | 1877.59 | 2808.12 | 2229.95 | 1793.15 | 2925.13 | 2469.35 | 2033.93 | 3426.53 | 2919.45 | 2539.44 |
| Q(true)/Q(exp) | 1.16 | **0.98** | 0.86 | 1.13 | **0.94** | 0.80 | 1.17 | **1.04** | 0.91 | 1.45 | 1.30 | **1.20** |

547

548
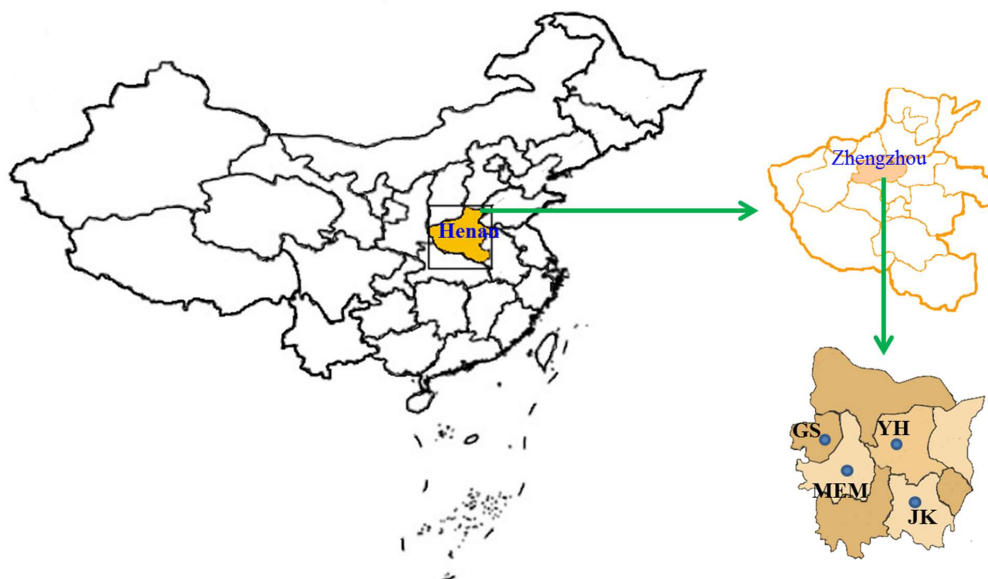
549

550    Fig 1. Map of Zhengzhou, China showing the locations of sampling sites.

551

Atmospheric
Chemistry
and Physics
Discussions

552
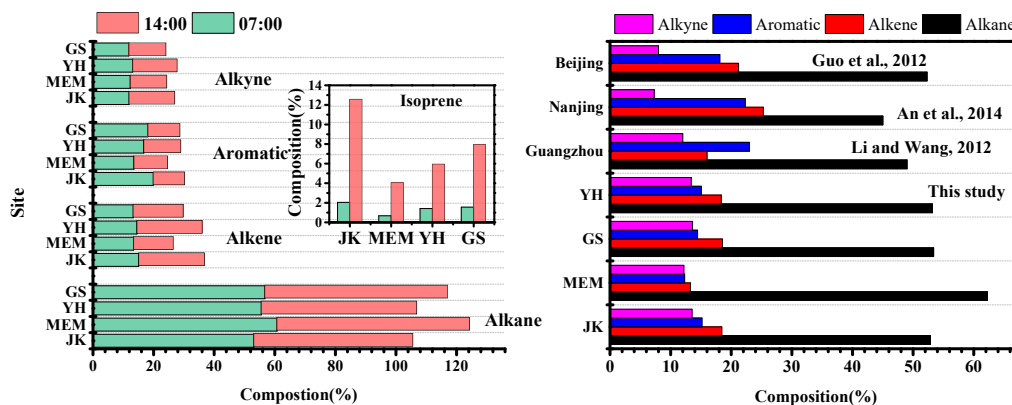


Fig 2. Compositions of major organic classes and comparison between Zhengzhou and

other cities in China

Atmospheric
Chemistry
and Physics
Discussions
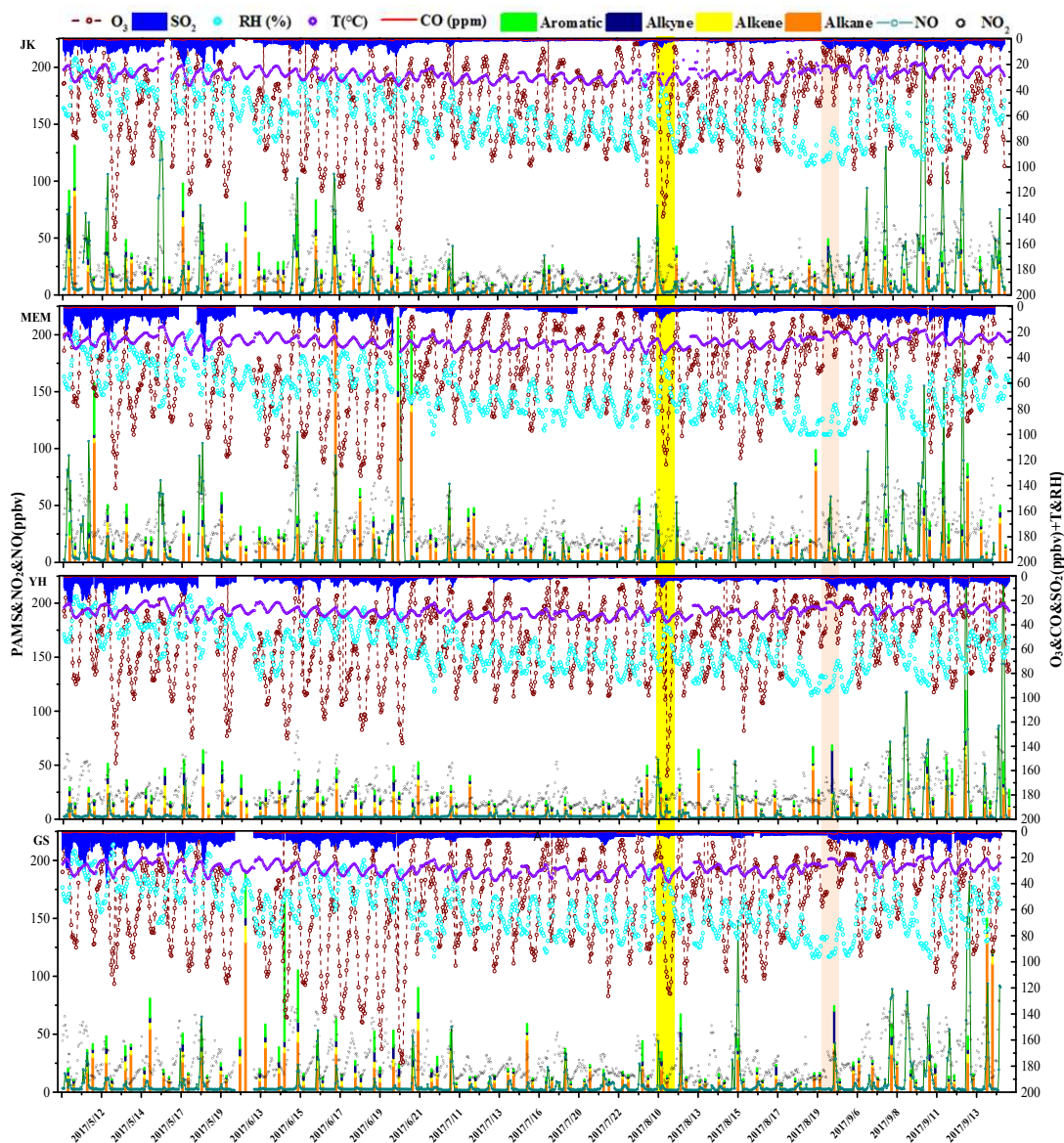


553

554

555    Fig 3. Temporal variations of mixing ratios of PAMS, CO, SO₂, NO, NO₂ and O₃ and

556    meteorological conditions at each site. 10ᵗʰ of August and 5ᵗʰ of September are highlighted as

557    yellow and pink, respectively.

558
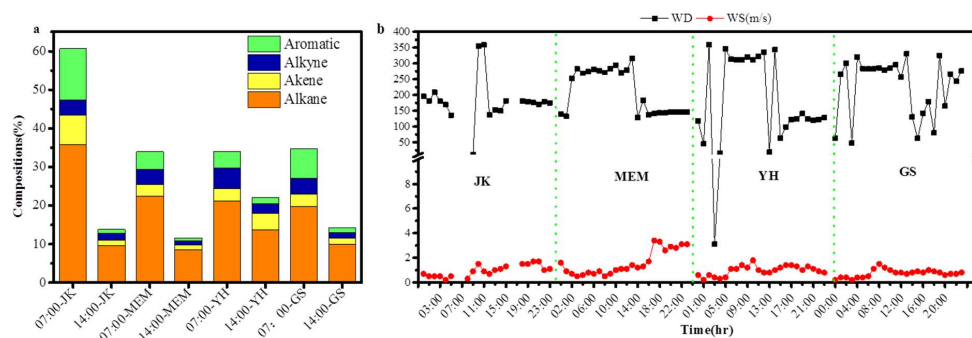
560      Fig.4. Temporal variation of compositions, wind direction and wind speed on 10th of August 2017

565

566
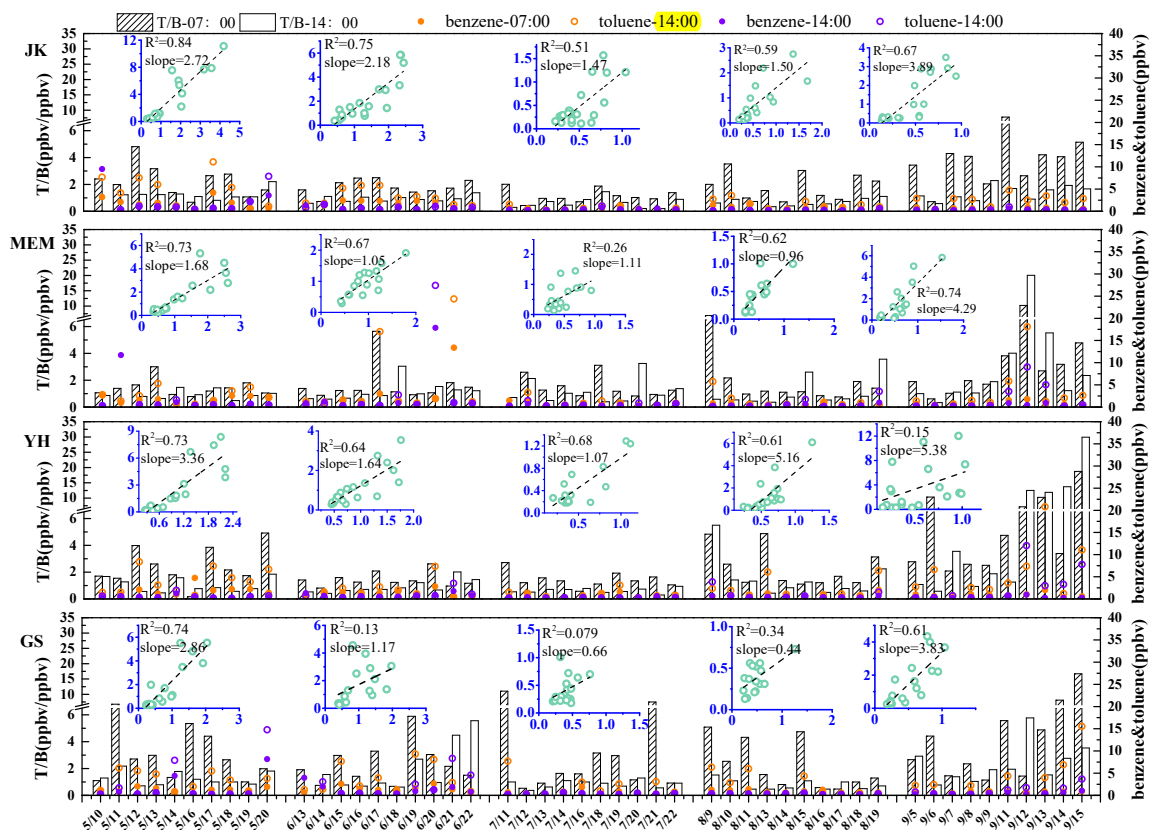
Fig 5. Time series of benzene and toluene and the correlation analysis between these two

compounds at every site

**Note:** The vertical axis in every small figure represents the mixing ratio of toluene (ppbv), while

the horizontal axis stands for benzene level (ppbv).

571

Atmospheric
Chemistry
and Physics
Discussions
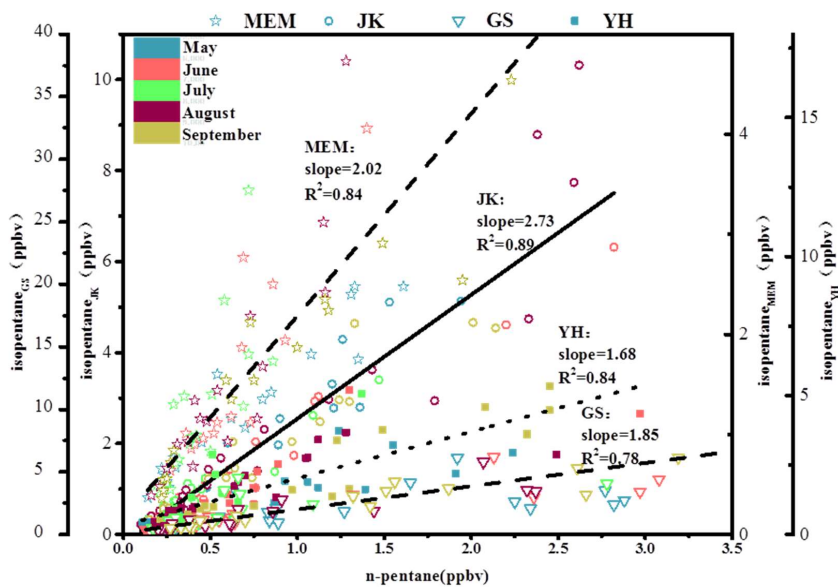
572



573        Fig 6. Ratios of isopentane to n-pentane at every site

574

575
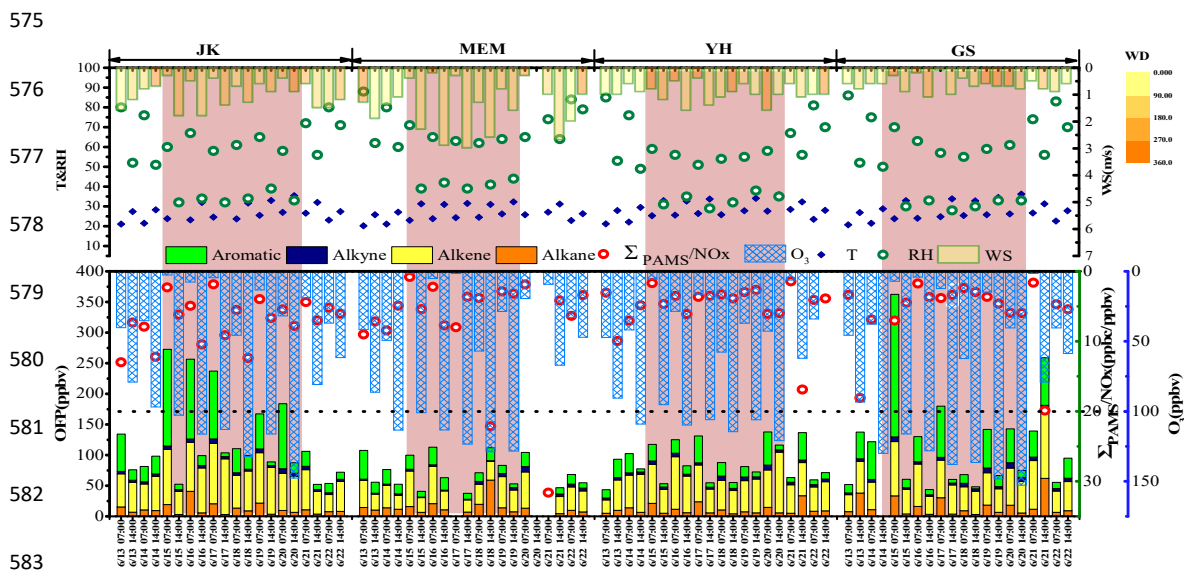


584    Fig 7. Spatio-temporal variations in meteorological factors, OFP of each organic group, $\Sigma_{PAMS}/NO_x$,

585            and mixing ratios of $O_3$ in June. Clear days at RH<45% are highlighted in pink.

586

Atmospheric
Chemistry
and Physics
Discussions
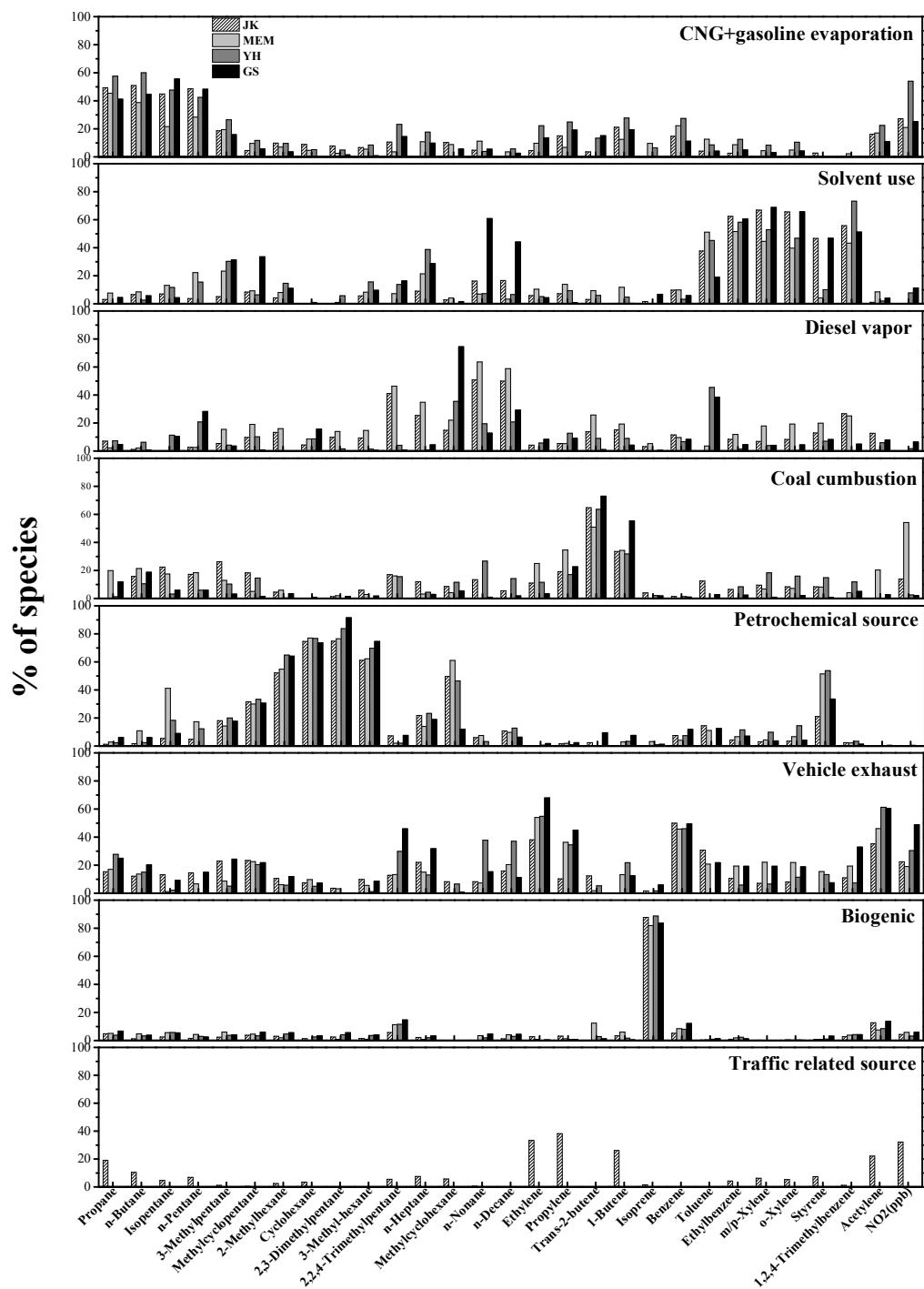
588                    Fig. 8 Explained variations in source profiles as identified by PMF

589
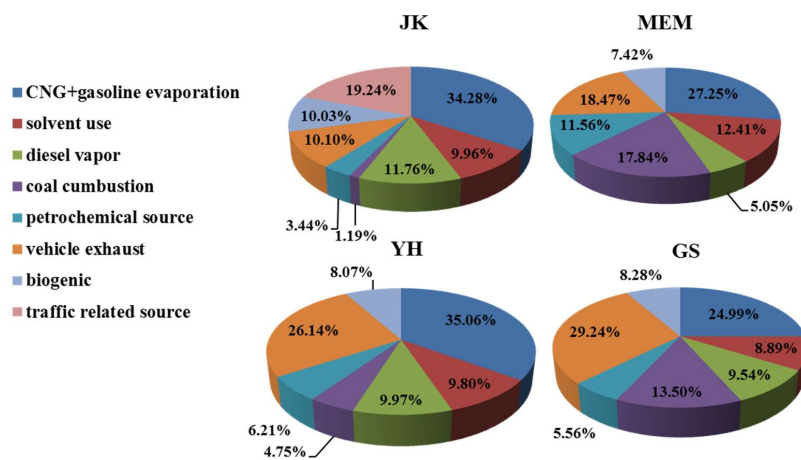


591                    Fig 9. Source apportionment results during the whole sampling period.

592

593

May

June

July

August

September
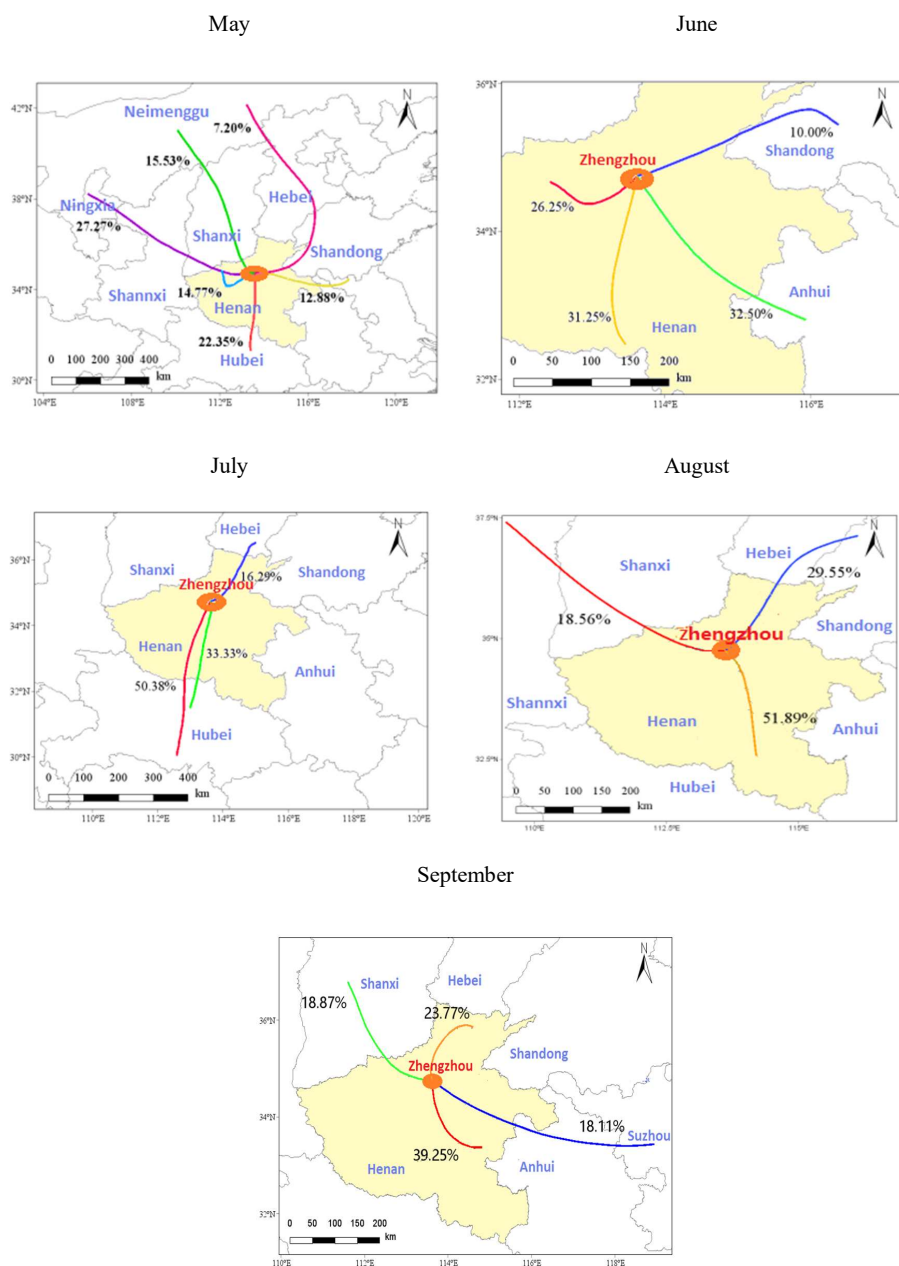


Fig 10. Cluster analysis of Zhengzhou in each sampling month

594

595

Atmospheric
Chemistry
and Physics
Discussions

596    **Ref.**

597    Abeleira, A., Pollack, I. B., Sive, B., Zhou, Y., Fischer, E. V., and Farmer, D. K.: Source characterization of volatile
598    organic compounds in the Colorado Northern Front Range Metropolitan Area during spring and summer 2015, Journal
599    of Geophysical Research: Atmospheres, 10.1002/2016jd026227, 2017.

600    Akagi, S. K., Yokelson, R. J., Wiedinmyer, C., Alvarado, M. J., Reid, J. S., Karl, T., Crounse, J. D., and Wennberg, P.
601    O.: Emission factors for open and domestic biomass burning for use in atmospheric models, Atmospheric Chemistry
602    and Physics, 11, 4039-4072, 10.5194/acp-11-4039-2011, 2011.

603    An, J., Zhu, B., Wang, H., Li, Y., Lin, X., and Yang, H.: Characteristics and source apportionment of VOCs measured
604    in an industrial area of Nanjing, Yangtze River Delta, China, Atmospheric Environment, 97, 206-214,
605    10.1016/j.atmosenv.2014.08.021, 2014.

606    Barletta, B., Meinardi, S., Sherwood Rowland, F., Chan, C.-Y., Wang, X., Zou, S., Yin Chan, L., and Blake, D. R.:
607    Volatile organic compounds in 43 Chinese cities, Atmospheric Environment, 39, 5979-5990,
608    10.1016/j.atmosenv.2005.06.029, 2005.

609    Blanchard, C. L., and Hidy, G. M.: Ozone Response to Emission Reductions in the Southeastern United States,
610    Atmospheric Chemistry and Physics Discussions, 1-33, 10.5194/acp-2017-534, 2017.

611    Capps, S. L., Hu, Y., and Russell, A. G.: Assessing Near-Field and Downwind Impacts of Reactivity-Based
612    Substitutions, Journal of the Air & Waste Management Association, 60, 316-327, 10.3155/1047-3289.60.3.316, 2012.

613    Carter, W.P.L.: Updated maximum incremental reactivity scale and hydrocarbon bin reactivities for regulatory
614    applications, Prepared for California Air Resources Board Contract 07-339, 2010.

615    Chen, S.-P., Liu, T.-H., Chen, T.-F., Yang, C.-F. O., Wang, J.-L., and Chang, J. S.: Diagnostic Modeling of PAMS
616    VOC Observation, Environ. Sci. Technol., 44, 4635–4644, 2010.

617    Chen, W. T., Shao, M., Lu, S. H., Wang, M., Zeng, L. M., Yuan, B., and Liu, Y.: Understanding primary and secondary
618    sources of ambient carbonyl compounds in Beijing using the PMF model, Atmospheric Chemistry and Physics, 14,
619    3047-3062, 10.5194/acp-14-3047-2014, 2014.

620    Cheng, L., Fu, L., Angle, R. P., and Sandhu, H. S.: Seasonal variations of volatile organic compounds in Edmonton,
621    Alberta, Atmospheric Environment, 31, 239-246, 1997.

622    Duan, J., Tan, J., Yang, L., Wu, S., and Hao, J.: Concentration, sources and ozone formation potential of volatile
623    organic compounds (VOCs) during ozone episode in Beijing, Atmospheric Research, 88, 25-35,
624    10.1016/j.atmosres.2007.09.004, 2008.

625    Gao, W., Tie, X., Xu, J., Huang, R., Mao, X., Zhou, G., and Chang, L.: Long-term trend of O3 in a mega City
626    (Shanghai), China: Characteristics, causes, and interactions with precursors, The Science of the total environment,
627    603-604, 425-433, 10.1016/j.scitotenv.2017.06.099, 2017.

628    Geddes, J. A., Murphy, J. G., and Wang, D. K.: Long term changes in nitrogen oxides and volatile organic compounds
629    in Toronto and the challenges facing local ozone control, Atmospheric Environment, 43, 3407-3415,
630    10.1016/j.atmosenv.2009.03.053, 2009.

631    Geng, F., Zhang, Q., Tie, X., Huang, M., Ma, X., Deng, Z., Yu, Q., Quan, J., and Zhao, C.: Aircraft measurements of
632    O3, NOx, CO, VOCs, and SO2 in the Yangtze River Delta region, Atmospheric Environment, 43, 584-593,
633    10.1016/j.atmosenv.2008.10.021, 2009.

634    Geng, N., Wang, J., Xu, Y., Zhang, W., Chen, C., and Zhang, R.: PM2.5 in an industrial district of Zhengzhou, China:
635    Chemical composition and source apportionment, Particuology, 11, 99-109, 10.1016/j.partic.2012.08.004, 2013.

Atmospheric
Chemistry
and Physics
Discussions

636   Gentner, D. R., Worton, D. R., Isaacman, G., Davis, L. C., Dallmann, T. R., Wood, E. C., Herndon, S. C., Goldstein, A.

637   H., and Harley, R. A.: Chemical composition of gas-phase organic carbon emissions from motor vehicles and

638   implications for ozone production, Environmental science & technology, 47, 11837-11848, 10.1021/es401470e, 2013.

639   Gilman, J. B., Lerner, B. M., Kuster, W. C., and de Gouw, J. A.: Source signature of volatile organic compounds from

640   oil and natural gas operations in northeastern Colorado, Environmental science & technology, 47, 1297-1305,

641   10.1021/es304119a, 2013.

642   Gong, M., Yin, S., Gu, X., Xu, Y., Jiang, N., and Zhang, R.: Refined 2013-based vehicle emission inventory and its

643   spatial and temporal characteristics in Zhengzhou, China, The Science of the total environment, 599-600, 1149-1159,

644   10.1016/j.scitotenv.2017.03.299, 2017.

645   Guo, H., Cheng, H. R., Ling, Z. H., Louie, P. K., and Ayoko, G. A.: Which emission sources are responsible for the

646   volatile organic compounds in the atmosphere of Pearl River Delta?, Journal of hazardous materials, 188, 116-124,

647   10.1016/j.jhazmat.2011.01.081, 2011.

648   Guo, H., Ling, Z. H., Cheng, H. R., Simpson, I. J., Lyu, X. P., Wang, X. M., Shao, M., Lu, H. X., Ayoko, G., Zhang, Y.

649   L., Saunders, S. M., Lam, S. H. M., Wang, J. L., and Blake, D. R.: Tropospheric volatile organic compounds in China,

650   The Science of the total environment, 574, 1021-1043, 10.1016/j.scitotenv.2016.09.116, 2017.

651   Guo, S., Tan, J., Duan, J., Ma, Y., Yang, F., He, K., and Hao, J.: Characteristics of atmospheric non-methane

652   hydrocarbons during haze episode in Beijing, China, Environmental monitoring and assessment, 184, 7235-7246,

653   10.1007/s10661-011-2493-9, 2012.

654   Han, D., Gao, S., Fu, Q., Cheng, J., Chen, X., Xu, H., Liang, S., Zhou, Y., and Ma, Y.: Do volatile organic compounds

655   (VOCs) emitted from petrochemical industries affect regional PM 2.5 ?, Atmospheric Research, 209, 123-130,

656   10.1016/j.atmosres.2018.04.002, 2018.

657   Hidy, G. M., and Blanchard, C. L.: Precursor reductions and ground-level ozone in the Continental United States,

658   Journal of the Air & Waste Management Association, 65, 1261-1282, 10.1080/10962247.2015.1079564, 2015.

659   Ho, K. F., Lee, S. C., Ho, W. K., Blake, D. R., Cheng, Y., Li, Y. S., Ho, S. S. H., Fung, K., Louie, P. K. K., and Park,

660   D.: Vehicular emission of volatile organic compounds (VOCs) from a tunnel study in Hong Kong, Atmos. Chem. Phys.,

661   9, 7491–7504, 2009.

662   Hoque, R. R., Khillare, P. S., Agarwal, T., Shridhar, V., and Balachandran, S.: Spatial and temporal variation of BTEX

663   in the urban atmosphere of Delhi, India, The Science of the total environment, 392, 30-40,

664   10.1016/j.scitotenv.2007.08.036, 2008.

665   Huang, C., Wang, H. L., Li, L., Wang, Q., Lu, Q., de Gouw, J. A., Zhou, M., Jing, S. A., Lu, J., and Chen, C. H.: VOC

666   species and emission inventory from vehicles and their SOA formation potentials estimation in Shanghai, China,

667   Atmospheric Chemistry and Physics, 15, 11081-11096, 10.5194/acp-15-11081-2015, 2015a.

668   Huang, X., Zhang, Y., Yang, W., Huang, Z., Wang, Y., Zhang, Z., He, Q., Lü, S., Huang, Z., Bi, X., and Wang, X.:

669   Effect of traffic restriction on reducing ambient volatile organic compounds (VOCs): Observation-based evaluation

670   during a traffic restriction drill in Guangzhou, China, Atmospheric Environment, 161, 61-70,

671   10.1016/j.atmosenv.2017.04.035, 2017.

672   Huang, Y., Ling, Z. H., Lee, S. C., Ho, S. S. H., Cao, J. J., Blake, D. R., Cheng, Y., Lai, S. C., Ho, K. F., Gao, Y., Cui,

673   L., and Louie, P. K. K.: Characterization of volatile organic compounds at a roadside environment in Hong Kong: An

674   investigation of influences after air pollution control strategies, Atmospheric Environment, 122, 809-818,

675   10.1016/j.atmosenv.2015.09.036, 2015b.

676   Iannuzzi, A., Verga, M. C., Renis, M., Schiavo, A., Salvatore, V., Santoriello, C., Pazzano, D., Licenziati, M. R., and

677   Polverino, M.: Air pollution and carotid arterial stiffness in children, Cardiology in the young, 20, 186-190,

678   10.1017/S1047951109992010, 2010.

Atmospheric
Chemistry
and Physics
Discussions

679    IARC: IARC (International Agency for Research on Cancer) Monographs on the Evaluation of Carcinogenic Risks to

680    Human. http://monographs.iarc.fr/ENG/Classification/latest_classif.php. (Accessed on 13 December 2017)

681    Jia, C., Mao, X., Huang, T., Liang, X., Wang, Y., Shen, Y., Jiang, W., Wang, H., Bai, Z., Ma, M., Yu, Z., Ma, J., and

682    Gao, H.: Non-methane hydrocarbons (NMHCs) and their contribution to ozone formation potential in a petrochemical

683    industrialized city, Northwest China, Atmospheric Research, 169, 225-236, 10.1016/j.atmosres.2015.10.006, 2016.

684    Jin, X., and Holloway, T.: Spatial and temporal variability of ozone sensitivity over China observed from the Ozone

685    Monitoring Instrument, Journal of Geophysical Research: Atmospheres, 120, 7229-7246, 10.1002/2015jd023250, 2015.

686    Jobson, B. T., Parrish, D. D., Goldan, P., Kuster, W., Fehsenfeld, F. C., Blake, D. R., Blake, N. J., and Niki, H.: Spatial

687    and temporal variability of nonmethane hydrocarbon mixing ratios and their relation to photochemical lifetime, Journal

688    of Geophysical Research: Atmospheres, 103, 13557-13567, 10.1029/97jd01715, 1998.

689    Jobson, B. T., Berkowitz, C. M., Kuster, W. C., Goldan, P. D., Williams, E. J., Fesenfeld, F. C., Apel, E. C., Karl, T.,

690    Lonneman, W. A., and Riemer, D.: Hydrocarbon source signatures in Houston, Texas: Influence of the petrochemical

691    industry, Journal of Geophysical Research, 109, 10.1029/2004jd004887, 2004.

692    Langford, A. O., Senff, C. J., Alvarez, R. J., Banta, R. M., and Hardesty, R. M.: Long-range transport of ozone from the

693    Los Angeles Basin: A case study, Geophysical Research Letters, 37, n/a-n/a, 10.1029/2010gl042507, 2010.

694    Lau, A. K., Yuan, Z., Yu, J. Z., and Louie, P. K.: Source apportionment of ambient volatile organic compounds in

695    Hong Kong, The Science of the total environment, 408, 4138-4149, 10.1016/j.scitotenv.2010.05.025, 2010.

696    Li, B., Ho, S. S. H., Xue, Y., Huang, Y., Wang, L., Cheng, Y., Dai, W., Zhong, H., Cao, J., and Lee, S.:

697    Characterizations of volatile organic compounds (VOCs) from vehicular emissions at roadside environment: The first

698    comprehensive study in Northwestern China, Atmospheric Environment, 161, 1-12, 10.1016/j.atmosenv.2017.04.029,

699    2017a.

700    Li, K., Chen, L., Ying, F., White, S. J., Jang, C., Wu, X., Gao, X., Hong, S., Shen, J., Azzi, M., and Cen, K.:

701    Meteorological and chemical impacts on ozone formation: A case study in Hangzhou, China, Atmospheric Research,

702    10.1016/j.atmosres.2017.06.003, 2017b.

703    Li, K., Li, J., Wang, W., Tong, S., Liggio, J., and Ge, M.: Evaluating the effectiveness of joint emission control policies

704    on the reduction of ambient VOCs: Implications from observation during the 2014 APEC summit in suburban Beijing,

705    Atmospheric Environment, 164, 117-127, 10.1016/j.atmosenv.2017.05.050, 2017c.

706    Li, L., and Wang, X.: Seasonal and diurnal variations of atmospheric non-methane hydrocarbons in Guangzhou, China,

707    International journal of environmental research and public health, 9, 1859-1873, 10.3390/ijerph9051859, 2012.

708    Li, L., Chen, Y., Zeng, L., Shao, M., Xie, S., Chen, W., Lu, S., Wu, Y., and Cao, W.: Biomass burning contribution to

709    ambient volatile organic compounds (VOCs) in the Chengdu–Chongqing Region (CCR), China, Atmospheric

710    Environment, 99, 403-410, 10.1016/j.atmosenv.2014.09.067, 2014.

711    Li, Q., Zhang, L., Wang, T., Wang, Z., Fu, X., and Zhang, Q.: "New" Reactive Nitrogen Chemistry Reshapes the

712    Relationship of Ozone to Its Precursors, Environmental science & technology, 52, 2810-2818, 10.1021/acs.est.7b05771,

713    2018.

714    Lin, X., Traner, M., and Liu, S. C.: On the Nonlinearity of the Tropospheric Ozone Production, Journal Of Geophysical

715    Research, 93, 15879-15888, 1998.

716    Liu, B., Liang, D., Yang, J., Dai, Q., Bi, X., Feng, Y., Yuan, J., Xiao, Z., Zhang, Y., and Xu, H.: Characterization and

717    source apportionment of volatile organic compounds based on 1-year of observational data in Tianjin, China,

718    Environmental pollution, 218, 757-769, 10.1016/j.envpol.2016.07.072, 2016a.

719    Liu, C., Zhang, C., Mu, Y., Liu, J., and Zhang, Y.: Emission of volatile organic compounds fromdomestic coal stove

720    with the actual alternation of flaming and smoldering combustion processes, Environmental Pollution,

721    10.1016/j.envpol.2016.11.089, 2016b.

Atmospheric
Chemistry
and Physics
Discussions

722     Liu, C., Ma, Z., Mu, Y., Liu, J., Zhang, C., Zhang, Y., Liu, P., and Zhang, H.: The levels, variation characteristics, and

723     sources of atmospheric non-methane hydrocarbon compounds during wintertime in Beijing, China, Atmospheric

724     Chemistry and Physics, 17, 10633-10649, 10.5194/acp-17-10633-2017, 2017.

725     Liu, H., Liu, S., Xue, B., Lv, Z., Meng, Z., Yang, X., Xue, T., Yu, Q., and He, K.: Ground-level ozone pollution and its

726     health impacts in China, Atmospheric Environment, 173, 223-230, 10.1016/j.atmosenv.2017.11.014, 2018.

727     Liu, Y., Shao, M., Fu, L., Lu, S., Zeng, L., and Tang, D.: Source profiles of volatile organic compounds (VOCs)

728     measured in China: Part I, Atmospheric Environment, 42, 6247-6260, 10.1016/j.atmosenv.2008.01.070, 2008a.

729     Liu, Y., Shao, M., Lu, S., Chang, C.-C., Wang, J.-L., and Fu, L.: Source apportionment of ambient volatile organic

730     compounds in the Pearl River Delta, China: Part II, Atmospheric Environment, 42, 6261-6274,

731     10.1016/j.atmosenv.2008.02.027, 2008b.

732     Liu, Y., Yuan, B., Li, X., Shao, M., Lu, S., Li, Y., Chang, C. C., Wang, Z., Hu, W., Huang, X., He, L., Zeng, L., Hu, M.,

733     and Zhu, T.: Impact of pollution controls in Beijing on atmospheric oxygenated volatile organic compounds (OVOCs)

734     during the 2008 Olympic Games: observation and modeling implications, Atmospheric Chemistry and Physics, 15,

735     3045-3062, 10.5194/acp-15-3045-2015, 2015.

736     Louie, P. K. K., Ho, J. W. K., Tsang, R. C. W., Blake, D. R., Lau, A. K. H., Yu, J. Z., Yuan, Z., Wang, X., Shao, M.,

737     and Zhong, L.: VOCs and OVOCs distribution and control policy implications in Pearl River Delta region, China,

738     Atmospheric Environment, 76, 125-135, 10.1016/j.atmosenv.2012.08.058, 2013.

739     Luecken, D. J., Napelenok, S. L., Strum, M., Scheffe, R., and Phillips, S.: Sensitivity of Ambient Atmospheric

740     Formaldehyde and Ozone to Precursor Species and Source Types Across the United States, Environmental science &

741     technology, 52, 4668-4675, 10.1021/acs.est.7b05509, 2018.

742     Lyu, X. P., Chen, N., Guo, H., Zhang, W. H., Wang, N., Wang, Y., and Liu, M.: Ambient volatile organic compounds

743     and their effect on ozone production in Wuhan, central China, The Science of the total environment, 541, 200-209,

744     10.1016/j.scitotenv.2015.09.093, 2016.

745     Malley, C. S., Braban, C. F., Dumitrean, P., Cape, J. N., and Heal, M. R.: The impact of speciated VOCs on regional

746     ozone increment derived from measurements at the UK EMEP supersites between 1999 and 2012, Atmospheric

747     Chemistry and Physics, 15, 8361-8380, 10.5194/acp-15-8361-2015, 2015.

748     McGaughey, G. R., Desai, N. R., Allen, D. T., Seila, R. L., Lonneman, W. A., Fraser, M. P., Harley, R. A., Pollack, A.

749     K., Ivy, J. M., and Price, J. H.: Analysis of motor vehicle emissions in a Houston tunnel during the Texas Air Quality

750     Study 2000, Atmospheric Environment, 38, 3363-3372, 10.1016/j.atmosenv.2004.03.006, 2004.

751     Millet, D. B., Baasandorj, M., Hu, L., Mitroo, D., Turner, J., and Williams, B. J.: Nighttime Chemistry and Morning

752     Isoprene Can Drive Urban Ozone Downwind of a Major Deciduous Forest, Environmental science & technology, 50,

753     4335-4342, 10.1021/acs.est.5b06367, 2016.

754     Monod, A., Sive, B. C., Avino, P., Chen, T., Blake, D. R., and Rowland, F. S.: Monoaromatic compounds in ambient

755     air of various cities: a focus on correlations between the xylenes and ethylbenzene, Atmospheric Environment, 35,

756     135-149, 2001.

757     Na, K., Kim, Y. P., Moon, K.-C., Moon, I., and Fung, K.: Concentrations of volatile organic compounds in an industrial

758     area of Korea, Atmospheric Environment 35, 2747-2756, 2001.

759     Nagashima, T., Sudo, K., Akimoto, H., Kurokawa, J., and Ohara, T.: Long-term change in the source contribution to

760     surface ozone over Japan, Atmospheric Chemistry and Physics, 17, 8231-8246, 10.5194/acp-17-8231-2017, 2017.

761     Ou, J., Zheng, J., Li, R., Huang, X., Zhong, Z., Zhong, L., and Lin, H.: Speciated OVOC and VOC emission inventories

762     and their implications for reactivity-based ozone control strategy in the Pearl River Delta region, China, The Science of

763     the total environment, 530-531, 393-402, 10.1016/j.scitotenv.2015.05.062, 2015.

764   Ou, J., Yuan, Z., Zheng, J., Huang, Z., Shao, M., Li, Z., Huang, X., Guo, H., and Louie, P. K.: Ambient Ozone Control
765   in a Photochemically Active Region: Short-Term Despiking or Long-Term Attainment?, Environmental science &
766   technology, 50, 5720-5728, 10.1021/acs.est.6b00345, 2016.
767   Paatero, P., and Tapper, U.: Positive matrix factorization: a non-negative Factor model with optimal utilization of Error
768   estimates of data values, Environmetrics, 5, 111-126, 1994.
769   Paatero, P.: Least squares formulation of robust non-negative factor analysis, Chemometrics and Intelligent Laboratory
770   Systems, 37, 23–35, 1997.
771   Paatero, P.: User's Guide for positive Matrix Factorization programs PMF2 and PMF3, part 1-2: Tutorial, 19 -21.
772   University of Helsinki, Helsinki, Finland, 2007.
773   Pal, S., Xueref-Remy, I., Ammoura, L., Chazette, P., Gibert, F., Royer, P., Dieudonné, E., Dupont, J. C., Haeffelin, M.,
774   Lac, C., Lopez, M., Morille, Y., and Ravetta, F.: Spatio-temporal variability of the atmospheric boundary layer depth
775   over the Paris agglomeration: An assessment of the impact of the urban heat island intensity, Atmospheric Environment,
776   63, 261-275, 10.1016/j.atmosenv.2012.09.046, 2012.
777   Polissar, A. V., Hopke, P. K., Paatero, P., Malm, W. C., and Sisler, J. F.: Atmospheric aerosol over Alaska: 2.
778   Elemental composition and sources, Journal of Geophysical Research: Atmospheres, 103, 19045-19057,
779   10.1029/98jd01212, 1998.
780   Pollack, I. B., Ryerson, T. B., Trainer, M., Neuman, J. A., Roberts, J. M., and Parrish, D. D.: Trends in ozone, its
781   precursors, and related secondary oxidation products in Los Angeles, California: A synthesis of measurements from
782   1960 to 2010, Journal of Geophysical Research: Atmospheres, 118, 5893-5911, 10.1002/jgrd.50472, 2013.
783   Raysoni, A. U., Stock, T. H., Sarnat, J. A., Chavez, M. C., Sarnat, S. E., Montoya, T., Holguin, F., and Li, W. W.:
784   Evaluation of VOC concentrations in indoor and outdoor microenvironments at near-road schools, Environmental
785   pollution, 231, 681-693, 10.1016/j.envpol.2017.08.065, 2017.
786   Russo, R. S., Zhou, Y., White, M. L., Mao, H., Talbot, R., and Sive, B. C.: Multi-year (2004–2008) record of
787   nonmethane hydrocarbons and halocarbons in New England: seasonal variations and regional sources, Atmospheric
788   Chemistry and Physics, 10, 4909-4929, 10.5194/acp-10-4909-2010, 2010.
789   Sahu, L. K., Tripathi, N., and Yadav, R.: Contribution of biogenic and photochemical sources to ambient VOCs during
790   winter to summer transition at a semi-arid urban site in India, Environmental pollution, 229, 595-606,
791   10.1016/j.envpol.2017.06.091, 2017.
792   Shao, M., Lu, S., Liu, Y., Xie, X., Chang, C., Huang, S., and Chen, Z.: Volatile organic compounds measured in
793   summer in Beijing and their role in ground-level ozone formation, Journal of Geophysical Research, 114,
794   10.1029/2008jd010863, 2009.
795   Shao, M., Wang, B., Lu, S., Yuan, B., and Wang, M.: Effects of Beijing Olympics Control Measures on Reducing
796   Reactive Hydrocarbon Species, Environ. Sci. Technol., 45, 514-519, 2011.
797   Shao, P., An, J., Xin, J., Wu, F., Wang, J., Ji, D., and Wang, Y.: Source apportionment of VOCs and the contribution to
798   photochemical ozone formation during summer in the typical industrial area in the Yangtze River Delta, China,
799   Atmospheric Research, 176-177, 64-74, 10.1016/j.atmosres.2016.02.015, 2016.
800   Shen, F., Ge, X., Hu, J., Nie, D., Tian, L., and Chen, M.: Air pollution characteristics and health risks in Henan
801   Province, China, Environmental research, 156, 625-634, 10.1016/j.envres.2017.04.026, 2017.
802   Simon, H., Reff, A., Wells, B., Xing, J., and Frank, N.: Ozone trends across the United States over a period of
803   decreasing NOx and VOC emissions, Environmental science & technology, 49, 186-195, 10.1021/es504514z, 2015.
804   Streets, D. G., Fu, J. S., Jang, C. J., Hao, J., He, K., Tang, X., Zhang, Y., Wang, Z., Li, Z., Zhang, Q., Wang, L., Wang,
805   B., and Yu, C.: Air quality during the 2008 Beijing Olympic Games, Atmospheric Environment, 41, 480-492,
806   10.1016/j.atmosenv.2006.08.046, 2007.

807    Sun, J., Wang, Y., Wu, F., Tang, G., Wang, L., Wang, Y., and Yang, Y.: Vertical characteristics of VOCs in the lower

808    troposphere over the North China Plain during pollution periods, Environmental pollution, 236, 907-915,

809    10.1016/j.envpol.2017.10.051, 2018.

810    Tang, J. H., Chan, L. Y., Chan, C. Y., Li, Y. S., Chang, C. C., Liu, S. C., Wu, D., and Li, Y. D.: Characteristics and

811    diurnal variations of NMHCs at urban, suburban, and rural sites in the Pearl River Delta and a remote site in South

812    China, Atmospheric Environment, 41, 8620-8632, 10.1016/j.atmosenv.2007.07.029, 2007.

813    Toro, M. V., Cremades, L. V., and Calbo, J.: Relationship between VOC and NOx emissions and chemical production

814    of tropospheric ozone in the Aburra Valley (Colombia), Chemosphere, 65, 881-888,

815    10.1016/j.chemosphere.2006.03.013, 2006.

816    Tsai, S. M., Zhang, J. J., Smith, K. R., Ma, Y., Rasmussen, R. A., and Khalil, M. A. K.: Characterization of

817    Non-methane Hydrocarbons Emitted from Various Cookstoves Used in China, Environ. Sci. Technol., 37, 2869-2877,

818    2003.

819    U.S.EPA: Revisions to the California state implementation plan and revision to the definition of volatile organic

820    compounds (VOC): removal of VOC exemptions for California's aerosol coating products reactivity-based regulation,

821    Fed. Regist. 70, 53930–53935, 2005.

822    US EPA: EPA Positive Matrix Factorization (PMF) 5.0 Fundamentals and User Guide,

823    http://www.epa.gov/heasd/documents/ EPA. PMF.5.0.User.Guide. pdf, 2014.

824    Wang, H.-l., Jing, S.-a., Lou, S.-r., Hu, Q.-y., Li, L., Tao, S.-k., Huang, C., Qiao, L.-p., and Chen, C.-h.: Volatile

825    organic compounds (VOCs) source profiles of on-road vehicle emissions in China, The Science of the total

826    environment, 607-608, 253-261, 10.1016/j.scitotenv.2017.07.001, 2017a.

827    Wang, H., Qiao, Y., Chen, C., Lu, J., Qiao, L., and Lou, S.: Source Profiles and Chemical Reactivity of Volatile

828    Organic Compounds from Solvent Use in Shanghai, China, Aerosol and Air Quality Research,

829    10.4209/aaqr.2013.03.0064, 2014.

830    Wang, H., Xiang, Z., Wang, L., Jing, S., Lou, S., Tao, S., Liu, J., Yu, M., Li, L., Lin, L., Chen, Y., Wiedensohler, A.,

831    and Chen, C.: Emissions of volatile organic compounds (VOCs) from cooking and their speciation: A case study for

832    Shanghai with implications for China, The Science of the total environment, 10.1016/j.scitotenv.2017.10.098, 2017b.

833    Wang, H. L., Chen, C. H., Wang, Q., Huang, C., Su, L. Y., Huang, H. Y., Lou, S. R., Zhou, M., Li, L., Qiao, L. P., and

834    Wang, Y. H.: Chemical loss of volatile organic compounds and its impact on the source analysis through a two-year

835    continuous measurement, Atmospheric Environment, 80, 488-498, 10.1016/j.atmosenv.2013.08.040, 2013a.

836    Wang, M., Shao, M., Lu, S.-H., Yang, Y.-D., and Chen, W.-T.: Evidence of coal combustion contribution to ambient

837    VOCs during winter in Beijing, Chinese Chemical Letters, 24, 829-832, 10.1016/j.cclet.2013.05.029, 2013b.

838    Wang, M., Shao, M., Chen, W., Lu, S., Liu, Y., Yuan, B., Zhang, Q., Zhang, Q., Chang, C. C., Wang, B., Zeng, L., Hu,

839    M., Yang, Y., and Li, Y.: Trends of non-methane hydrocarbons (NMHC) emissions in Beijing during 2002–2013,

840    Atmospheric Chemistry and Physics, 15, 1489-1502, 10.5194/acp-15-1489-2015, 2015.

841    Wang, T., Xue, L., Brimblecombe, P., Lam, Y. F., Li, L., and Zhang, L.: Ozone pollution in China: A review of

842    concentrations, meteorological influences, chemical precursors, and effects, The Science of the total environment, 575,

843    1582-1596, 10.1016/j.scitotenv.2016.10.081, 2017c.

844    Wang, X.-m., Sheng, G.-y., Fu, J.-m., Chan, C.-y., Lee, S.-C., Chan, L. Y., and Wang, Z.-s.: Urban roadside aromatic

845    hydrocarbons in three cities of the Pearl River Delta, People's Republic of China, Atmospheric Environment, 36, 5141–

846    5148, 2002.

847    Wang, Y., Guo, H., Zou, S., Lyu, X., Ling, Z., Cheng, H., and Zeren, Y.: Surface O3 photochemistry over the South

848    China Sea: Application of a near-explicit chemical mechanism box model, Environmental pollution, 234, 155-166,

849    10.1016/j.envpol.2017.11.001, 2018.

Atmospheric
Chemistry
and Physics
Discussions

Open Access

850  Wei, W., Cheng, S., Li, G., Wang, G., and Wang, H.: Characteristics of ozone and ozone precursors (VOCs and NOx)

851  around a petroleum refinery in Beijing, China, Journal of Environmental Sciences, 26, 332-342,

852  10.1016/s1001-0742(13)60412-x, 2014.

853  Wu, R., and Xie, S.: Spatial Distribution of Ozone Formation in China Derived from Emissions of Speciated Volatile

854  Organic Compounds, Environmental science & technology, 51, 2574-2583, 10.1021/acs.est.6b03634, 2017.

855  Xue, Y., Ho, S. S. H., Huang, Y., Li, B., Wang, L., Dai, W., Cao, J., and Lee, S.: Source apportionment of VOCs and

856  their impacts on surface ozone in an industry city of Baoji, Northwestern China, Scientific Reports, 7, 9979,

857  10.1038/s41598-017-10631-4, 2017.

858  Yan, Y., Yang, C., Peng, L., Li, R., and Bai, H.: Emission characteristics of volatile organic compounds from coal-,

859  coal gangue-, and biomass-fired power plants in China, Atmospheric Environment, 143, 261-269,

860  10.1016/j.atmosenv.2016.08.052, 2016.

861  Yan, Y., Peng, L., Li, R., Li, Y., Li, L., and Bai, H.: Concentration, ozone formation potential and source analysis of

862  volatile organic compounds (VOCs) in a thermal power station centralized area: A study in Shuozhou, China,

863  Environmental pollution, 223, 295-304, 10.1016/j.envpol.2017.01.026, 2017.

864  Yuan, B., Shao, M., Lu, S., and Wang, B.: Source profiles of volatile organic compounds associated with solvent use in

865  Beijing, China, Atmospheric Environment, 44, 1919-1926, 10.1016/j.atmosenv.2010.02.014, 2010.

866  Yuan, B., Hu, W. W., Shao, M., Wang, M., Chen, W. T., Lu, S. H., Zeng, L. M., and Hu, M.: VOC emissions,

867  evolutions and contributions to SOA formation at a receptor site in eastern China, Atmospheric Chemistry and Physics,

868  13, 8815-8832, 10.5194/acp-13-8815-2013, 2013a.

869  Yuan, Z., Lau, A. K. H., Shao, M., Louie, P. K. K., Liu, S. C., and Zhu, T.: Source analysis of volatile organic

870  compounds by positive matrix factorization in urban and rural environments in Beijing, Journal of Geophysical

871  Research, 114, 10.1029/2008jd011190, 2009.

872  Yuan, Z., Zhong, L., Lau, A. K. H., Yu, J. Z., and Louie, P. K. K.: Volatile organic compounds in the Pearl River Delta:

873  Identification of source regions and recommendations for emission-oriented monitoring strategies, Atmospheric

874  Environment, 76, 162-172, 10.1016/j.atmosenv.2012.11.034, 2013b.

875  Zhang, J., Sun, Y., Wu, F., Sun, J., and Wang, Y.: The characteristics, seasonal variation and source apportionment of

876  VOCs at Gongga Mountain, China, Atmospheric Environment, 88, 297-305, 10.1016/j.atmosenv.2013.03.036, 2014.

877  Zhang, Z., Wang, X., Zhang, Y., Lu, S., Huang, Z., Huang, X., and Wang, Y.: Ambient air benzene at background sites

878  in China's most developed coastal regions: exposure levels, source implications and health risks, The Science of the

879  total environment, 511, 792-800, 10.1016/j.scitotenv.2015.01.003, 2015.

880  Zhao, Y., Nguyen, N. T., Presto, A. A., Hennigan, C. J., May, A. A., and Robinson, A. L.: Intermediate Volatility

881  Organic Compound Emissions from On-Road Diesel Vehicles: Chemical Composition, Emission Factors, and

882  Estimated Secondary Organic Aerosol Production, Environmental science & technology, 49, 11516-11526,

883  10.1021/acs.est.5b02841, 2015.

884  Zheng, H., Kong, S., Xing, X., Mao, Y., Hu, T., Ding, Y., Li, G., Liu, D., Li, S., and Qi, S.: One year monitoring of

885  volatile organic compounds (VOCs) from an oil-gas station in northwest China, Atmospheric Chemistry and Physics

886  Discussions, 1-57, 10.5194/acp-2017-828, 2017.

887  Zhu, Y., Yang, L., Kawamura, K., Chen, J., Ono, K., Wang, X., Xue, L., and Wang, W.: Contributions and source

888  identification of biogenic and anthropogenic hydrocarbons to secondary organic aerosols at Mt. Tai in 2014,

889  Environmental pollution, 220, 863-872, 10.1016/j.envpol.2016.10.070, 2017.

890